ELECTRICAL

ENGINEERING

N68-22732 (ACCESSION NUMBER) (THRU)
69 (PAGES) 1 (CODE)
NASA-CR-61737 (NASA CR OR TMX OR AD NUMBER) 09 (CATEGORY)
FACILITY FORM 602

AUBURN RESEARCH FOUNDATION

AUBURN UNIVERSITY

AUBURN, ALABAMA

THE DESIGN OF A SOLID-STATE SINGLE-ENDED SWITCHING DC TO DC CONVERTER

PREPARED BY

MICROWAVE RESEARCH LABORATORY

M. A. HONNELL, PROJECT LEADER

N68 22732

CONTRACT NAS8-11184

GEORGE C. MARSHALL SPACE FLIGHT CENTER

NATIONAL AERONAUTICS AND SPACE ADMINISTRATION

HUNTSVILLE, ALABAMA

APPROVED BY:

C H Holmes

C. H. Holmes
Head Professor
Electrical Engineering

SUBMITTED BY:

M. A. Honnell

M. A. Honnell
Professor
Electrical Engineering

FORWORD

This is a special technical report of one phase of a study conducted by the Electrical Engineering Department under the auspices of Auburn Research Foundation toward fulfillment of the requirements prescribed in NASA Contract NAS8-11184 to develop a converter to supply power to a frequency-modulated television transmitter for use in space vehicles. The theory and design of the solid-state single-ended switching dc to dc converter are presented. The converter provides a highly regulated, electrically isolated d-c voltage source.

ABSTRACT

This investigation is concerned with the development, design, and construction of a dc to dc converter to provide power for a television transmitter to be used in space vehicles. The converter is implemented with solid-state components and an isolation transformer used in a single-ended switching configuration.

The solid-state single-ended switching dc to dc converter is divided into seven distinct sections: (1) input filter, (2) starting circuit, (3) single-ended switching transformer circuit, (4) integrated control oscillator, (5) pi-filter, (6) series regulator, (7) output filter. The power stage of the converter is driven with a constant pulse-width, the frequency of which is inversely proportional to the output voltage. Since the system uses negative feedback, the output voltage is regulated. The series regulator is included to obtain a more precise regulation of the output voltage. The input and output filters are included to enhance the electromagnetic compatibility of the converter.

The theory and equations describing the operation of the converter are presented. The design equations of the isolation transformer are developed for the ideal case. The design of each section is discussed in detail and a circuit diagram is shown. A single-ended switching dc to dc converter was designed and constructed. The final design of the converter was assembled in a prototype electronic package. The prototype was subjected to electromagnetic compatibility tests and temperature tests. The results of the tests and the performance of the converter are presented.

The nominal input and output voltage of the converter is 28 Vdc. The output voltage remained within $\pm$ 0.325 percent of the nominal output voltage over the complete temperature range, complete load range, and complete input voltage range. The converter has a maximum d-c output impedance of 0.1021 ohms and maintained an overall operating efficiency of approximately 80 percent under all conditions of operation.

TABLE OF CONTENTS

LIST OF TABLES

LIST OF FIGURES

THE DESIGN OF A SOLID-STATE SINGLE-ENDED
SWITCHING DC TO DC CONVERTER

W. W. Agerton and M. A. Honnell

I. INTRODUCTION

For many applications a d-c voltage that is electrically isolated from the prime d-c power source is required. Isolation may be achieved by using an isolation transformer in conjunction with some form of oscillating circuitry. The transformer secondary voltage must then be rectified to produce the desired d-c voltage. Circuit configurations that provide such a d-c voltage are normally referred to as dc to dc converters.

This investigation is concerned with obtaining a dc to dc converter that will produce a highly-regulated, electrically-isolated 28 volts dc for use in space vehicles. The configuration selected to achieve the desired voltage is a solid-state single-ended switching dc to dc converter.

The solid-state single-ended switching dc to dc converter may be divided into seven distinct sections: (1) input filter, (2) starting circuit, (3) single-ended switching transformer circuit, (4) integrated control oscillator, (5) pi-filter, (6) series regulator, (7) output filter. The series regulator is included only where precise regulation is required. The input and output filters are included because of radio frequency interference requirements in space equipment. A block diagram of the converter is shown in Figure 1.

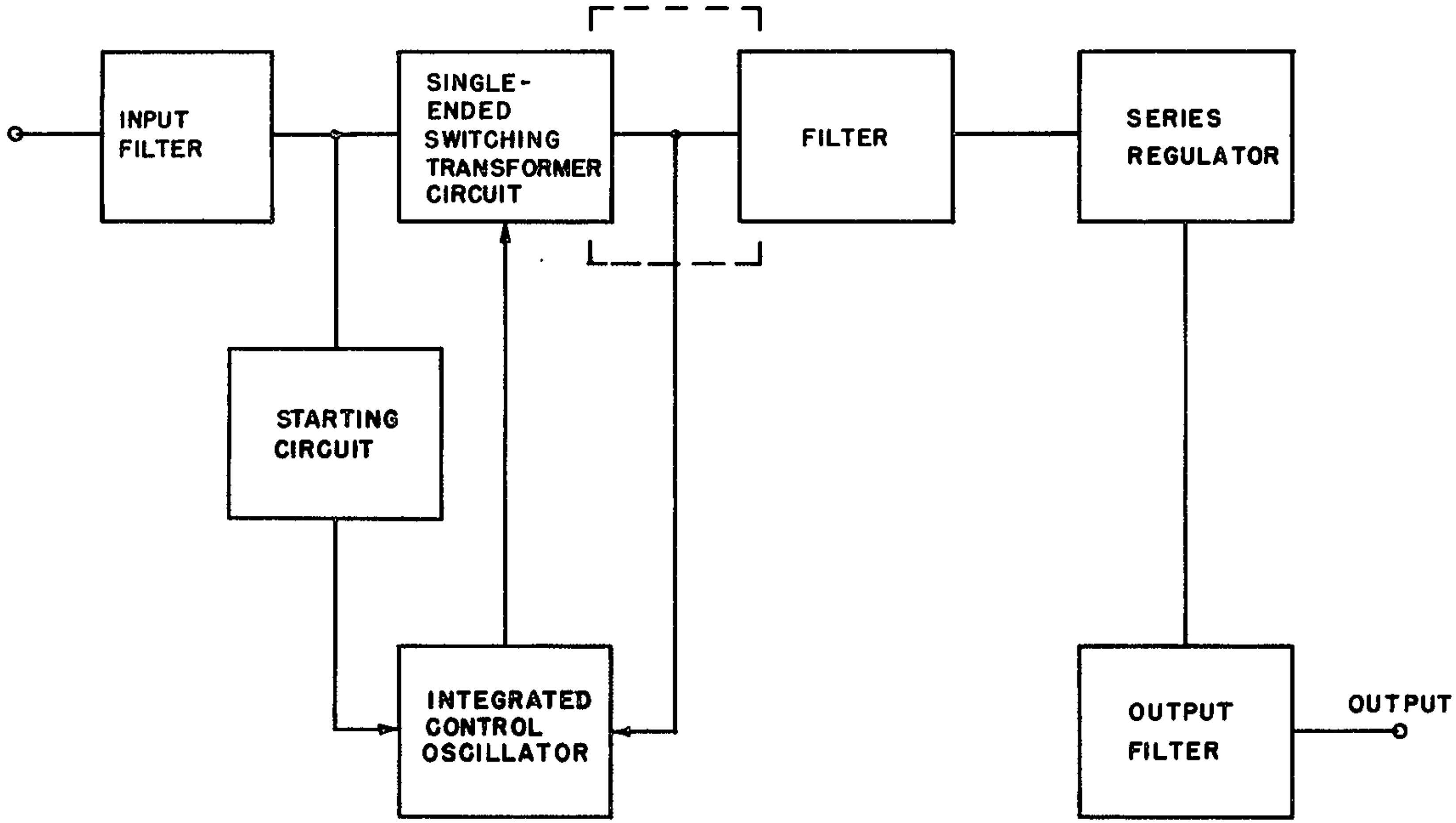

Fig. 1--Block Diagram of the Solid-State Single-ended Switching DC to DC Converter.

In such a converter, energy is first stored in the magnetic field through the primary circuitry of the isolation transformer.[1] The energy is then retrieved from the magnetic field through the secondary circuit and stored in a capacitor. It is then supplied to the load. It is most important to note that the energy storage cycle is complete before the energy retrieving cycle begins.

Each section of the converter is discussed in detail and a circuit diagram is presented. The design equations consider only the ideal case, and neglect transformer winding resistances and the voltage drops across saturated transistors.

II. THEORY OF OPERATION

A. Single-ended Switching Transformer Circuit

The basic diagram for the single-end switching transformer circuit is shown in Figure 2.

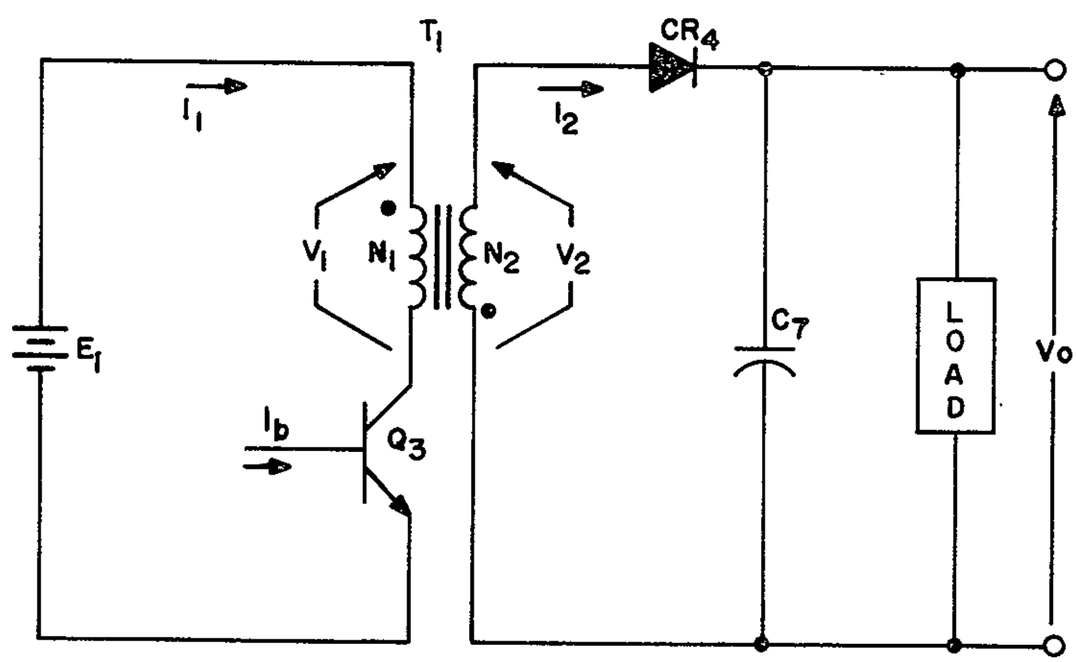

Fig. 2--Basic Diagram for the Single-ended Switching Transformer Circuit.

Waveforms associated with the switching circuit are shown in Figure 3. Transistor Q_3 is driven into saturation for a specific period of time, T_1, which causes the input voltage to appear across the primary winding,

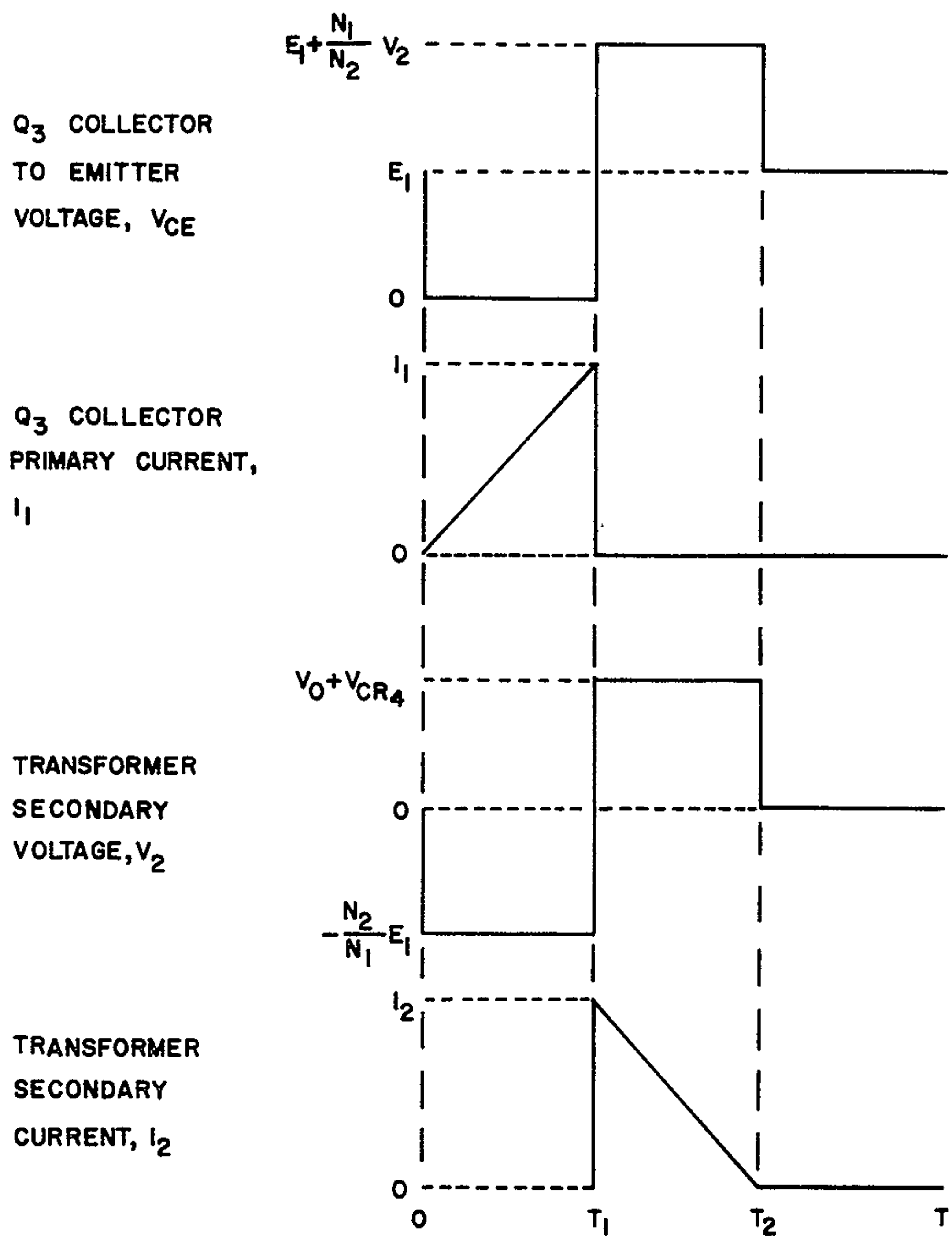

Fig. 3--Waveforms associated with the Single-ended Switching Transformer Circuit.

N_1, of transformer T_1. The voltage, V_2', induced in the secondary winding, N_2, during the time T_1 is expressed as

$$V_2' = \frac{N_2}{N_1} E_1 . \tag{1}$$

The secondary winding is phased as shown in Figure 2. This allows the diode, CR_4, to block current flow in the secondary winding during the time T_1. Since there is no power delivered by the transformer secondary winding during this time, the transformer may be treated as an inductor, as shown in the simplified diagram of Figure 4.

From Figure 4, the equation for the primary current, I_1, through transistor Q_3 may be calculated by using the equation

$$E_1 = L_1 \frac{di_1}{dt} \tag{2}$$

where L_1 is the inductance of the transformer primary winding. The primary current is then shown to be the integral of the voltage across the inductor and is given by

$$I_1 = \int_o^{T_1} \frac{E_1}{L_1} dt. \tag{3}$$

The magnetic material selected for use in the single-ended switching transformer can be shown to exhibit a constant inductance for a varying magnetomotive force. This is shown in Appendix A.

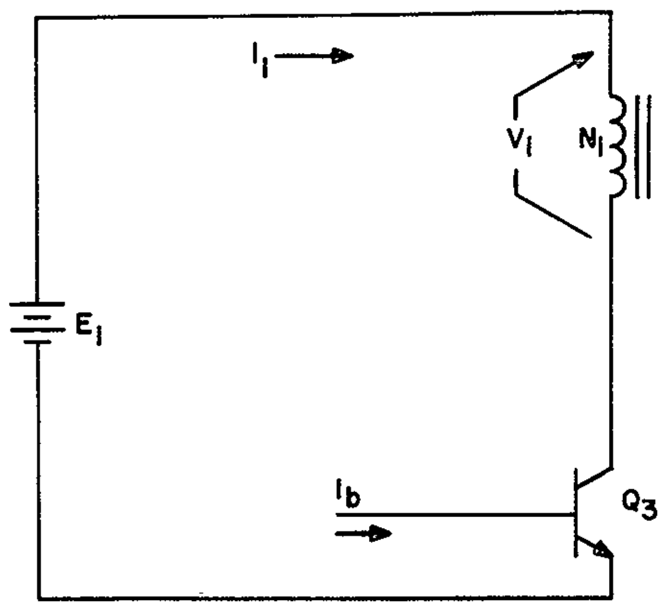

Fig. 4--Simplified Diagram for Time T_1.

The input voltage, E_1, is a constant; therefore, if inductance L_1 remains constant, then equation (3) may be written as

$$I_1 = \frac{E_1 T_1}{L_1} \tag{4}$$

Equation (4) shows that the peak transistor current is proportional to the time the transistor remains in saturation. It is most important to note that the peak collector current in the transistor is completely independent of the load, and is determined solely by the time T_1. Thus, by controlling the time T_1, the peak transistor current may be adjusted to correspond to a desired level within the capabilities of the transistor.

At time T_1, transistor Q_3 is driven into cutoff, which causes a reversal of the changing flux in the magnetic field of the transformer. The induced voltage in each winding is now of opposite polarity to the polarity during the time T_1. The diode, CR_4, is now forward-biased and current is allowed to flow in the secondary winding.

The voltage, V_2, induced in the secondary winding will be clamped to the sum of the output, V_o, and the forward voltage drop across the diode CR_4.

$$V_2 = V_o + V_{CR_4}. \tag{5}$$

V_o in this particular converter is controlled by feedback and is considered a constant. The diode voltage drop, V_{CR_4}, is also a constant.

The voltage, V_1, induced in the primary winding during the time (T_2-T_1) is given by

$$V_1 = \frac{N_1}{N_2} V_2 \ ; \tag{6}$$

or, substituting for V_2, V_1 becomes

$$V_1 = \frac{N_1}{N_2} (V_o + V_{CR_4}) \ . \tag{7}$$

The transistor collector-to-emitter voltage, V_{CE}, during the time (T_2-T_1) is seen to be the sum of the input voltage and the induced primary winding voltage.

$$V_{CE} = E_1 + V_1 \ . \tag{8}$$

Equation (7) may be substituted for V_1 to yield

$$V_{CE} = E_1 + \frac{N_1}{N_2} (V_o + V_{CR_4}) \ . \tag{9}$$

Care must be taken not to exceed the collector-to-emitter breakdown voltage of Q_3. Since E_1, V_o, and V_{CR_4} are relatively constant, equation (9) shows that the voltage across the collector-emitter terminals may be controlled by the proper selection of the turns ratio N_1/N_2. This will protect the transistor from secondary breakdown. However, equation (9) does not consider the low energy component stored in the leakage inductance of the transformer. This inductance will cause a voltage transient as transistor Q_3 is driven into the cutoff region. Under prolonged operation this could eventually cause a failure similar to secondary breakdown. To control the transient, a suppression network may be connected in parallel with the transformer primary winding.

During the time (T_2-T1), transistor Q_3 is in the cutoff region, and there is no current flow in the primary circuit. Since no energy is being stored by the magnetic field, the basic diagram of Figure 2 may be represented by the simplified diagram of Figure 5.

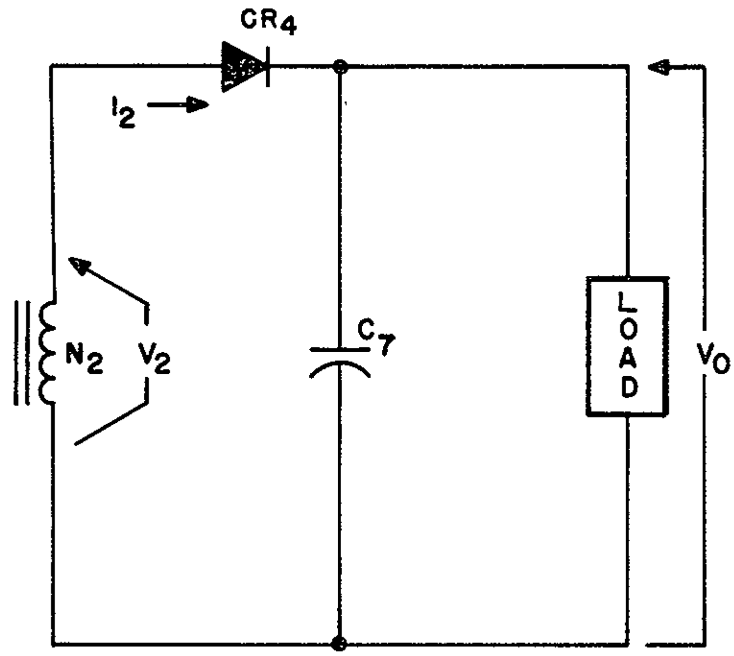

Fig. 5--Simplified Diagram for Time $(T_2 - T_1)$.

At time T_1, the energy, W_1, stored in the transformer magnetic field is given by the equation

$$W_1 = \frac{1}{2} L_1 I_1^2 . \tag{10}$$

The energy, W_2, delivered by the transformer during the time $(T_2 - T_1)$ is given by the equation

$$W_2 = \frac{1}{2} L_2 I_2^2 . \tag{11}$$

Since only the ideal case is being considered, the energy stored during time T_1 must equal the energy delivered during time (T_2-T_1). Equations (10) and (11) may be equated to determine the peak current, I_2, in the secondary winding at time T_1. I_2 is found to be

$$I_2 = \sqrt{\frac{L_1}{L_2}}\ I_1 \ . \tag{12}$$

For an ideal transformer[2],

$$\frac{L_1}{L_2} = \frac{{N_1}^2}{{N_2}^2} \tag{13}$$

Using equations (12) and (13), I_2 may be written as

$$I_2 = \frac{N_1}{N_2}\ I_1 \ . \tag{14}$$

Equation (14) shows that the peak current in the secondary winding is dependent only upon the peak primary current and the transformer turns ratio N_1/N_2.

The time (T_2-T_1) required to discharge the stored energy in the transformer magnetic field may be calculated from the equation

$$V_2 = L_2 \frac{di_2}{dt} \ . \tag{15}$$

From equation (15), I_2 is found to be

$$I_2 = \int_{T_1}^{T_2} \frac{V_2}{L_2}\, dt. \tag{16}$$

V_2 and L_2 are essentially constant because of the reasons given in the derivation of equations (4) and (5). I_2 may now be expressed as

$$I_2 = \frac{V_2}{L_2}\ (T_2 - T_1)\ , \tag{17}$$

and the discharge time (T_2-T_1) is given by

$$(T_2 - T_1) = \frac{I_2\ L_2}{V_2}\ . \tag{18}$$

The design equations for the single-ended switching transformer may be derived by assuming a maximum duty cycle of 50 percent for the power transistor Q_3. Consider time T_1 during which energy is stored in the magnetic field of the transformer. If a maximum duty cycle of 50 percent is desired, the voltage and current waveforms will be as shown in Figure 6. Note that the waveforms are shown only for the on time of the power transistor, Q_3.

The maximum average power that may be drawn from the source may be computed by integrating the instantaneous power[3] over the time interval T/2 and dividing by the period:

$$P = \frac{1}{T} \int_{0}^{T/2} e(t)i(t)dt\ , \tag{19}$$

where e(t)i(t) represents the instantaneous power. From Figure 6, e(t) is equal to E_1 which is a constant. The primary current i(t)

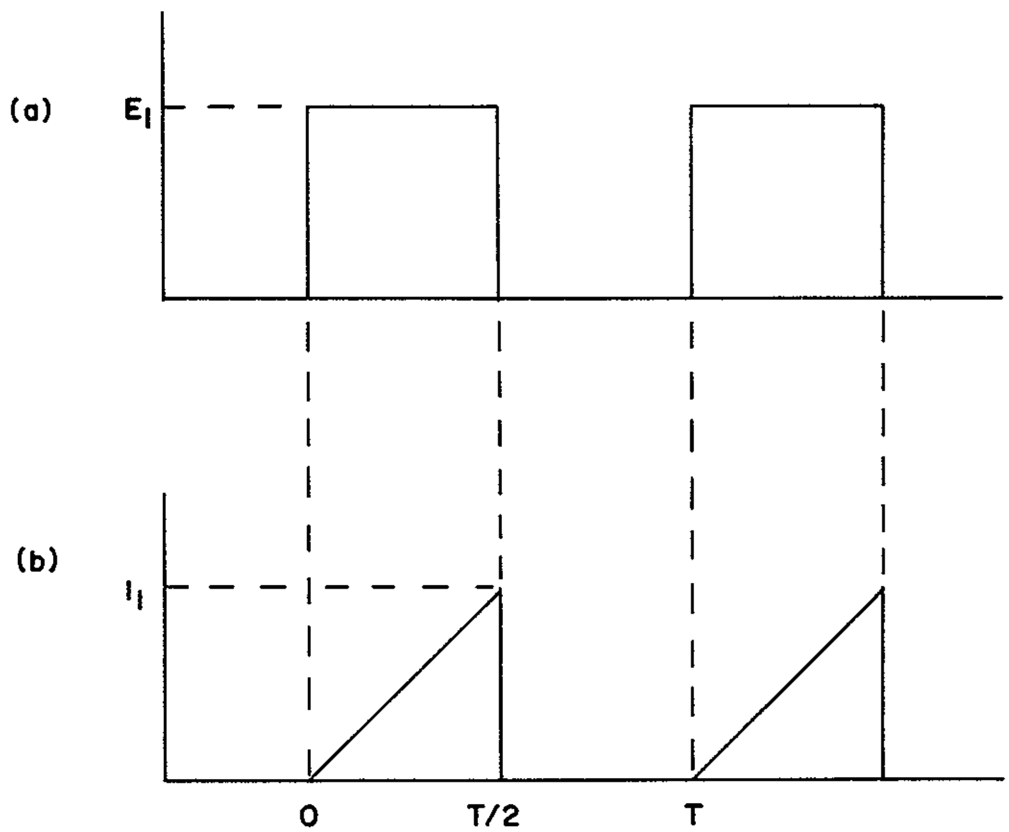

Fig. 6--Primary Winding Waveforms during Energy Storage Time for a 50-Percent Duty Cycle.

is found to be

$$i(t) = \frac{I_1 t}{T/2} \tag{20}$$

If e(t) and i(t) are substituted into equation (19), the power, P, is given as

$$P = \frac{1}{T} \int_0^{T/2} E_1 \frac{I_1 t}{T/2} dt \; . \tag{21}$$

The power is then found to be

$$P = \frac{E_1 I_1}{4} \; . \tag{22}$$

Equation (22) represents the theoretical maximum power that can be drawn from a source if Q_3 is restricted to a maximum duty cycle of 50 percent. This equation may be solved for I_1 to yield

$$I_1 = \frac{4P}{E_1} \tag{23}$$

I_1 is the peak current that must flow in the primary winding to stor sufficient energy to supply the required output power. The inductance needed to allow such a current peak may be calculated by using the equation

$$e(t) = L_1 \frac{di_1}{dt} \tag{24}$$

where $e(t)$ is equal to E_1. Equation (24) may be rearranged to yield

$$E_1 dt = L_1 di_1 \tag{25}$$

If both sides of equation (25) are integrated, L_1 is found to be

$$L_1 = \frac{E_1 T_1}{I_1} \tag{26}$$

The inductance of the magnetic material selected for use in the dc to dc converter is based on millihenries per 1000 turns[4]. The number of primary turns, N_1, may be calculated from the relationship[2]

$$\frac{N_1^{\,2}}{L_1} = \frac{N_k^{\,2}}{L_k} \tag{27}$$

where L_1 is the desired inductance of the primary winding and L_k is the known inductance per 1000 turns. Equation (27) may be solved to yield the number of primary turns N_1:

$$N_1 = \frac{1000}{\sqrt{\dfrac{L_k}{L_1}}} \tag{28}$$

Equations (23), (26), and (28) are needed to design the single-ended switching transformer. The actual design of the transformer is given later.

B. Starting Circuit

The purpose of the starting circuit is to provide a momentary voltage to the secondary circuitry of the isolation transformer T_1 of Figure 2. This voltage is used to start the integrated control oscillator.

The starting circuit is composed of a relaxation oscillator with a single-ended switching output stage. The relaxation oscillator uses an unijunction transistor biased in the negative resistance region to obtain astable operation[2]. The emitter of the unijunction is connected to an RC network in such a way that the firing voltage, V_p, is approached as the charge on the capacitor increases. When the unijunction fires, a pulse is applied to the base of the transistor in the output circuit. Energy is then transferred to the integrated control oscillator through a transformer.

C. Integrated Control Oscillator

The output voltage of the single-ended switching dc to dc converter may be precisely regulated by (1) controlling the operating frequency, (2) controlling the duty cycle of transistor Q_3, or (3) controlling both the operating frequency and the duty cycle of transistor Q_3. Controlling both the operating frequency and duty cycle is undesirable because of the complex circuitry involved and the increase in components. Controlling the duty cycle is undesirable for the same reasons but to a lesser extent. However, control of the operating frequency is less complicated and easily implemented.

To control the operating frequency, the on time of Q_3 is held constant while the period, T, is allowed to vary as the load varies.

For large power demands, T is small and the operating frequency is high. For small power demands, T is large, and the operating frequency is low. The frequency is thus modulated as a function of the load.

D. Series Regulator

The regulation of a d-c voltage can be expressed in terms of the various disturbances injected into the system. The most important of these are slow amplitude variations of the primary power source, a-c ripple from the voltage to be regulated, changes in the load current, and temperature variations which produce changes in the components comprising the regulator. The design intent of the series regulator is to minimize the effect of these disturbances. Regulators employing negative voltage feedback[5] serve very well to accomplish this. The basic block diagram for such a system is shown in Figure 7.

For purposes of feedback analysis, an equivalent circuit of the regulator is shown in Figure 8. E_o is the regulated output voltage, βE_o is the sample voltage, and E_1 is the difference between the sample voltage and the reference voltage E_{ref}:

$$E_1 = \beta E_o - E_{ref}. \tag{29}$$

The nominal gain of the amplifier from input to output is given by

$$K = \frac{E_o}{E_1} . \tag{30}$$

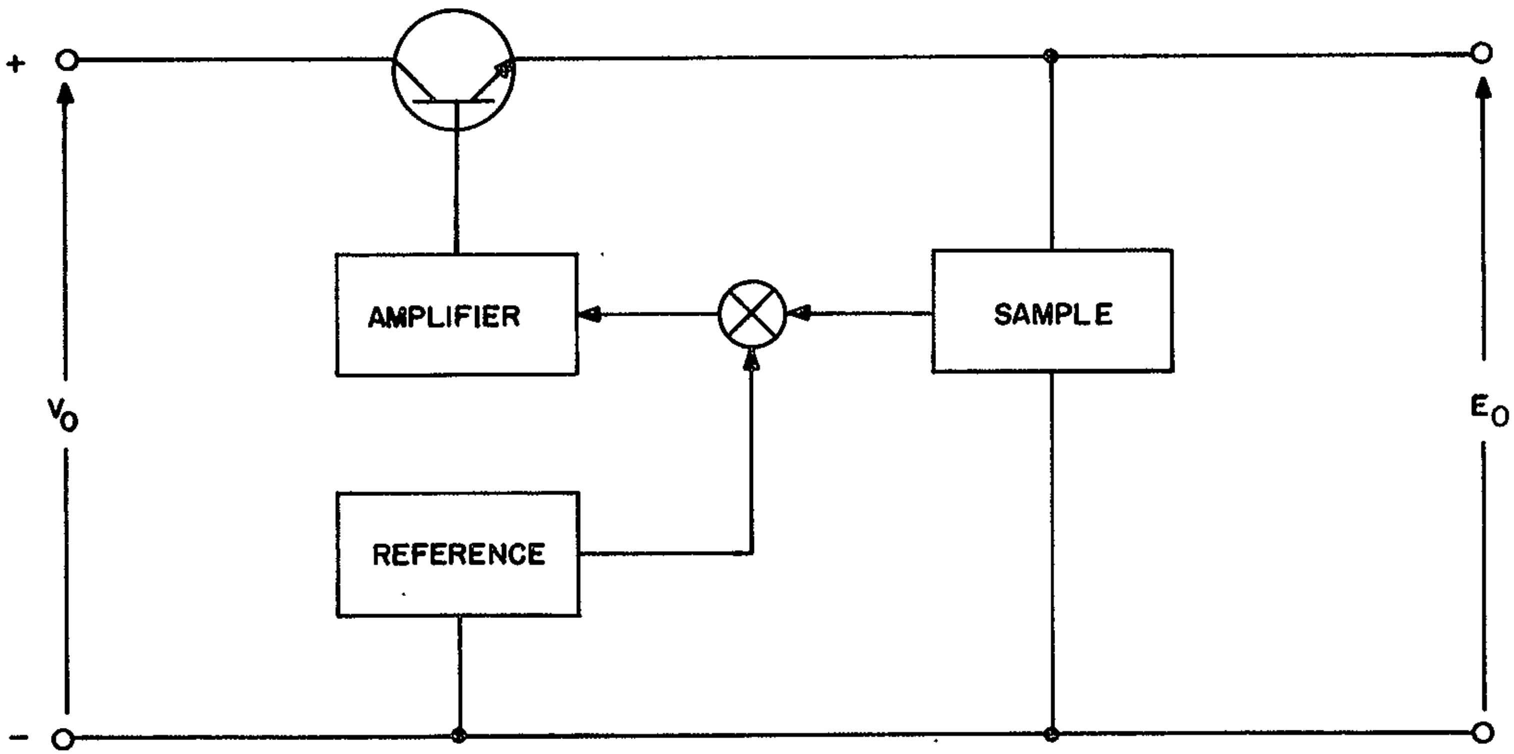

Fig. 7--Basic Block Diagram for a Series Regulator.

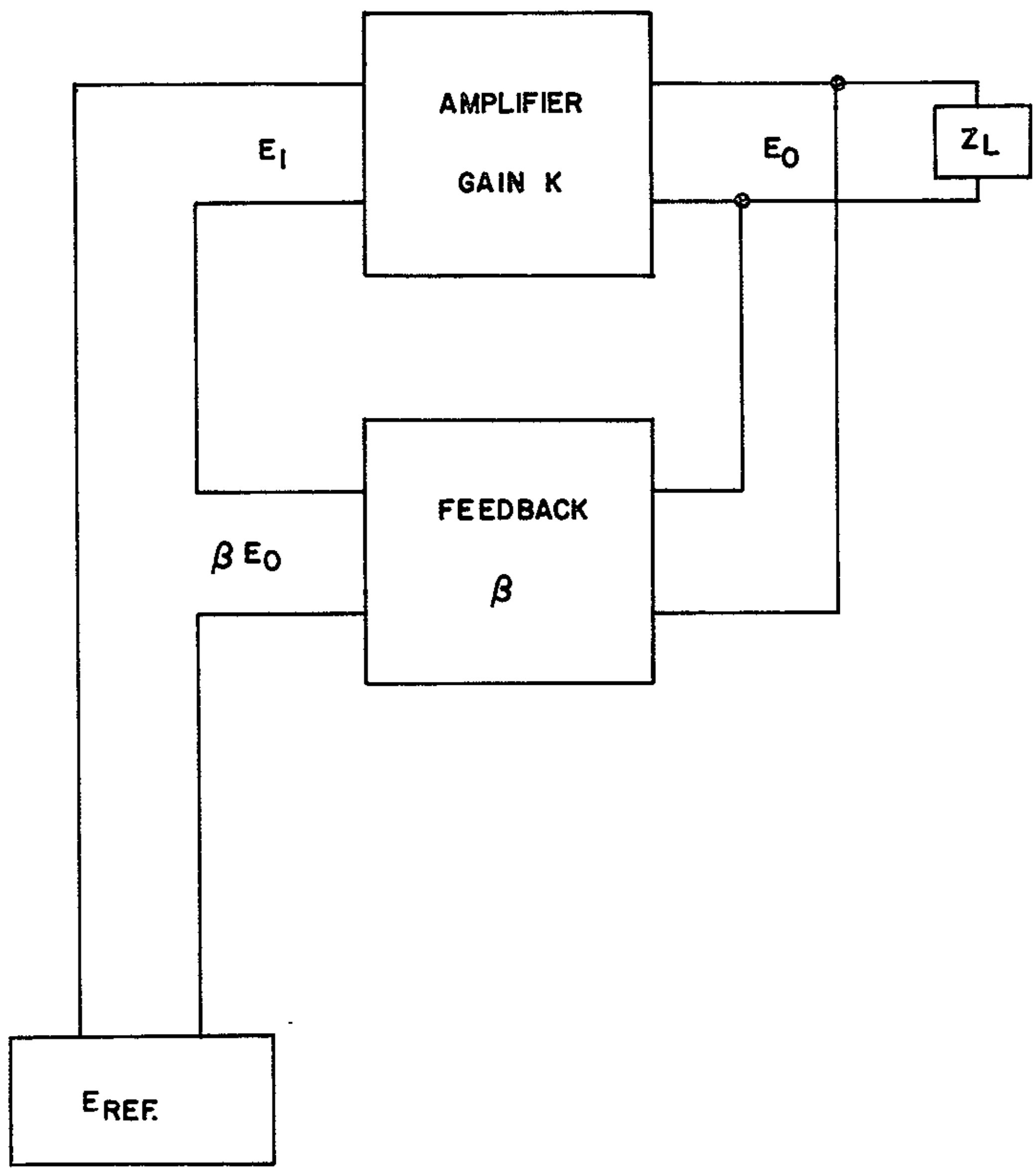

Fig. 8--Equivalent Feedback Circuit for a Series Regulator.

From equations (29) and (30) the following relationship may be found:

$$\frac{E_o}{E_{ref}} = \frac{-K}{1 - K\beta} \tag{31}$$

Equation (31) may be solved for E_o in terms of K, β, and E_{ref} to yield

$$E_o = \left(\frac{-K}{1 - K\beta}\right) E_{ref} \tag{32}$$

This equation expresses the output voltage variation of the feedback regulator in terms of the nominal gain K, the feedback fraction β, and the reference voltage changes. Here, the magnitude of the denominator becomes very important. If $|1 - K\beta|$ is less than unity, any change in reference voltage produces an amplified change in the output voltage. The feedback is positive and the circuit becomes regenerative. If $|1 - K\beta|$ is equal to zero, the gain becomes infinite, and the output will become unstable. If $|1 - K\beta|$ is greater than unity, the output voltage is less susceptible to reference voltage changes, temperature effects, and noise. The feedback is said to be negative and the circuit is degenerative.

It should now be realized that stability is of prime importance in the design of the series regulator. One of the best ways to correct unstable or regenerative regulators is to limit their high-frequency response by including a large capacitor across the output. This will provide the necessary high-frequency cutoff, and in addition, will serve to decrease the output impedance at high frequencies.

III. DESIGN OF THE CONVERTER

The design specifications for the single-ended switching dc to dc converter are listed below.

1. The input voltage shall vary from 24 to 32 volts with no degradation of the output.
2. The output voltage shall be 28 volts dc.
3. The maximum output current capacity shall be 1.4 amperes with a nominal output current of 1.0 ampere.
4. The output voltage regulation shall be $\pm$ 0.4 per cent for a load change of 0 to 1.4 amperes.
5. The output ripple shall not exceed 20 millivolts peak-to-peak over the complete input voltage variation with a load change of 0 to 1.4 amperes.
6. The output voltage spikes shall not exceed 40 millivolts peak-to-peak over the complete input voltage variation with a load change of 0 to 1.4 amperes.
7. The converter shall operate over a temperature range of -20 degrees C to + 85 degrees C without performance degradation.
8. The converter shall conform to the electromagnetic compatibility specifications in accordance with George C. Marshall Space Flight Center specification MSFC-SPEC-279 or MIL-I-6181D.

9. The output shall be electrically isolated from the input.

A. Single-ended Switching Transformer Circuit

To properly design a single-ended switching transformer circuit, the desired output power must be known. Also, an accurate estimation of converter efficiency must be obtainable. The overall efficiency of the single-ended switching dc to dc converter may be accurately estimated at 80 per cent. From the converter specifications, the desired output power, P_o, is found to be

$$P_o = (28)(1.4) = 39.2 \text{ watts} \tag{33}$$

The input power, P_1, required may be calculated by dividing the output power by the converter efficiency:

$$P_1 = \frac{39.2}{.8} = 49 \text{ watts} . \tag{34}$$

The single-ended switching transformer circuit is shown in Figure 9. The design equation

$$I_1 = \frac{4\ P_1}{E_1} \tag{35}$$

may be used to determine the collector current of Q_3 needed to produce an output power of 39.2 watts. In this equation the minimum input voltage of 24 volts dc must be used. I_1 is found to be 8.2 amperes.

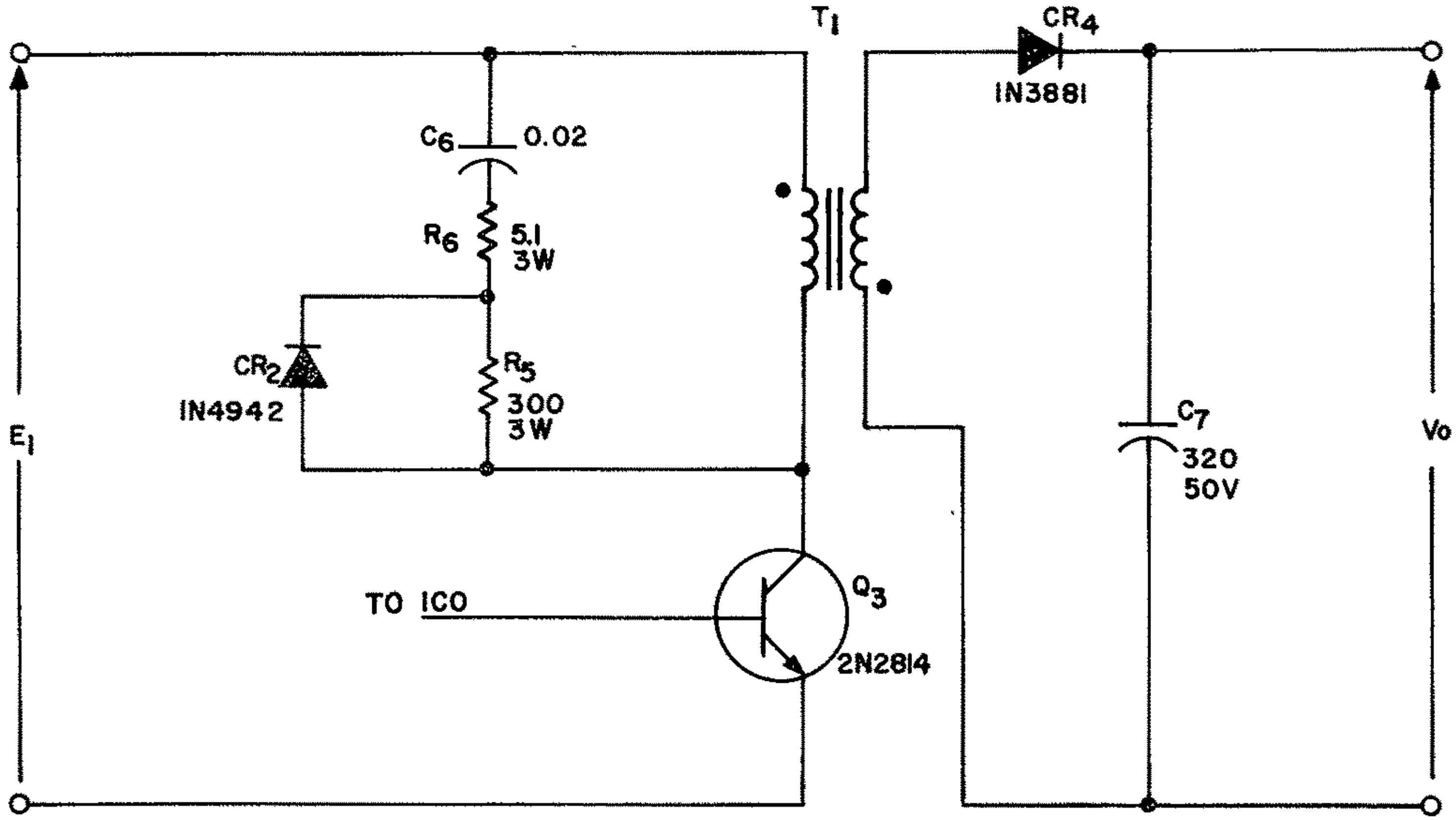

NOTE: ALL VALUES ARE IN OHMS, MICROFARADS, OR MICROHENRIES.

Fig. 9--Single-ended Switching Transformer Circuit.

The on time, T_1, of transistor Q_3 is selected to be 30 microseconds. T_1 is chosen by the designer and depends upon the desired maximum frequency of operation and the amount of power that must be supplied. T_1 should not be chosen too large to insure that the transformer core material does not saturate. For the core material selected, which is powdered permalloy with a permeability of 60, the on time may range from 20 to 60 microseconds.

The inductance required to allow a peak current flow of 8.2 amperes in the time T_1 may be calculated by using the design equation

$$L_1 = \frac{E_1 T_1}{I_1} \tag{36}$$

L_1 is found to be 88 microhenrys.

The primary winding, N_1, of transformer T_1 may be calculated by using the equation

$$N_1 = \frac{1000}{\sqrt{L_k/L_1}} \tag{37}$$

N_1 is found to be 38 turns.

To protect transistor Q_3 from secondary breakdown, the transformer secondary winding, N_2, is selected to be 38 turns.

A diagram of transformer T_1 is shown in Figure 10. Winding N_3 provides a low bias voltage for the series regulator.

The operating point of the transformer core may be determined by using the equation[4]

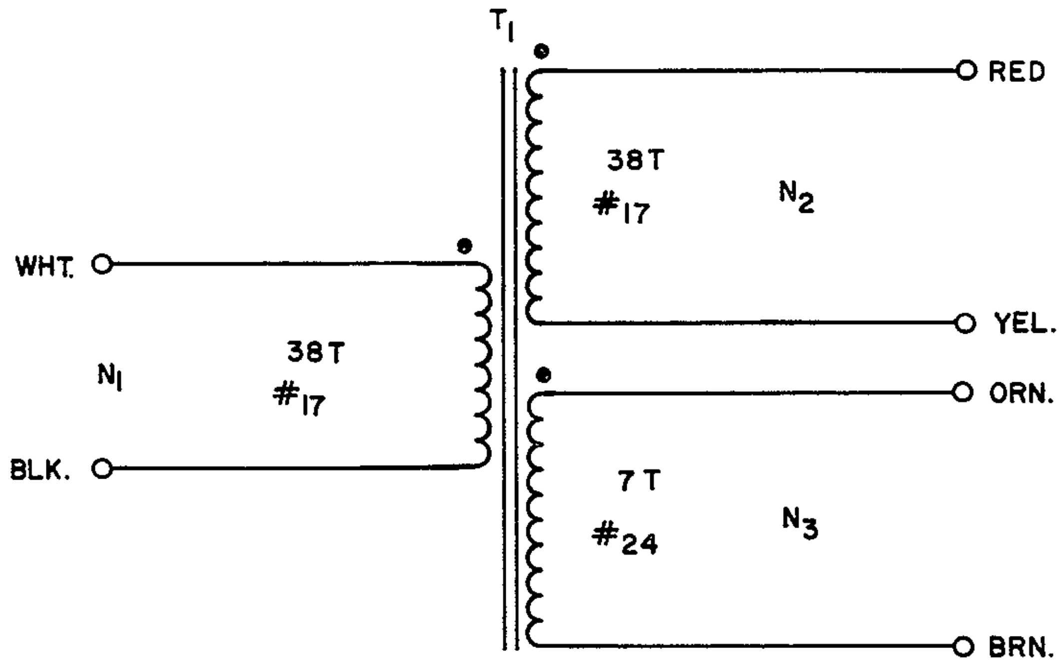

Figure 10--Winding Data for Transformer T_1.

$$H = \frac{.4\pi\ N_1 I_1}{ml} . \tag{38}$$

H is the magnetizing force in oersteds, I_1 is the peak current through the core winding, ml is the mean magnetic path length, and N_1 is the number of turns on the core. H is calculated to be 48.2 oersteds. The flux density, B, may be determined from the magnetization curves[4] of Figure 11. The value calculated for H is intersected with the 60μ curves. B is found to be approximately 2750 gausses. The operating point of the transformer core may now be determined as shown in Figure 12.[4]

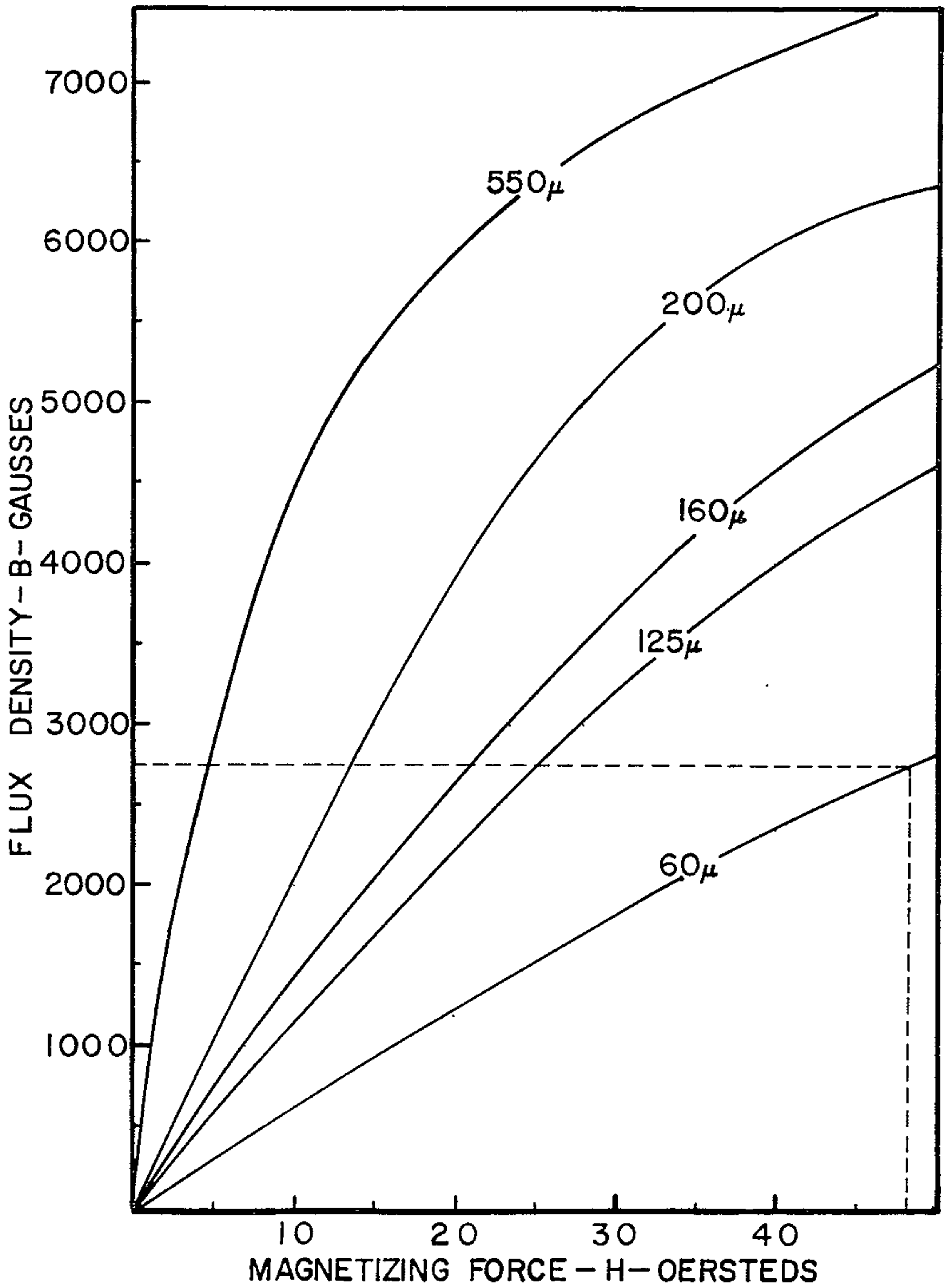

Fig. 11--Magnetization Curves for Powdered Permalloy.

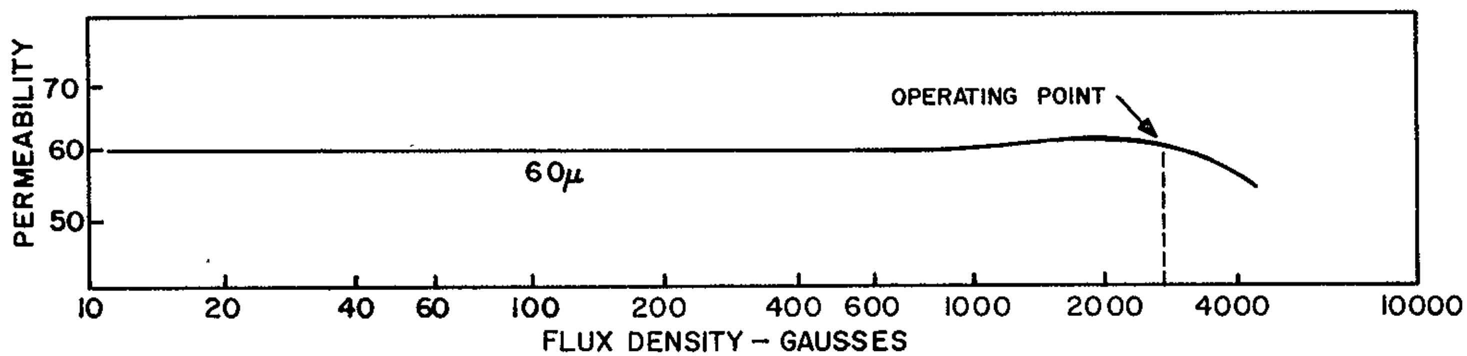

Fig. 12--Permeability vs Flux Density for Powdered Permalloy.

A suppression network is connected across the primary winding of the transformer as shown in Figure 9. This network will aid in protecting Q_3 by dissipating the low-energy component stored in the leakage inductance of the transformer. The network consists of resistors R_5 and R_6, capacitor C_6, and diode CR_2. The values for R_5, R_6, and C_6 are determined experimentally. The current capacity required for the diode, CR_2, is also determined experimentally.

The diode, CR_4, must be selected with the following characteristics

1. The minimum reverse breakdown voltage V_r must be

$$V_r \geqq \frac{N_2}{N_1} E_1 + V_o. \tag{39}$$

2. The diode must have a current capacity large enough to handle the peak forward secondary current I_2.
3. The diode must be capable of switching a current which decreases linearly from I_2 to 0 in time (T_2-T_1).

The output voltage ripple associated with the storage capacitor C_7 is produced by two factors. The product of the peak current through the capacitor and the equivalent series resistance of the capacitor will cause a slight increase in ripple. The ripple will be further increased because energy is repeatedly stored and retrieved from the capacitor. For a minimum output ripple, C_7 must be selected with a low dissipation factor. An inductor L_3 and capacitor C_{11} are added to form a pi-filter to further decrease the ripple.

B. Starting Circuit

The starting circuit shown in Figure 13 was designed to satisfy two conditions. First, the on time of the output transistor, Q_2, must be of sufficient duration to start the integrated control oscillator at the lower temperature limit of -20 degrees C. This was accomplished by selecting capacitor C_8 and resistor R_{26}. Second, the off time of Q_2 must be long compared to the on time of the power transistor Q_3 in the single-ended switching transformer circuit. This is accomplished by properly selecting resistor R_1.

The second condition above allows the use of a diode, CR_1, to inhibit the operation of the starting circuit. When transistor Q_3 is saturated, capacitor C_8 is discharged to ground through CR_1 and the starting circuit is not allowed to operate.

The RC network of R_3, R_4, and C_9 serves as a pulse-shaping network for the signal applied to the base of Q_2. C_9 also blocks the d-c component and allows Q_2 to operate in a switching mode. Transformer T_2 is designed in the same manner as transformer T_1 of Figure 9.

C. Integrated Control Oscillator

An astable multivibrator is used to control the operating frequency of the converter, and thus, regulate the output voltage. The multivibrator was implemented by using a μA709 integrated high performance operational amplifier[6].

The basic multivibrator configuration requires a positive and a negative input voltage. Since only a positive voltage is available, the basic circuit must be modified by providing a positive dc bias

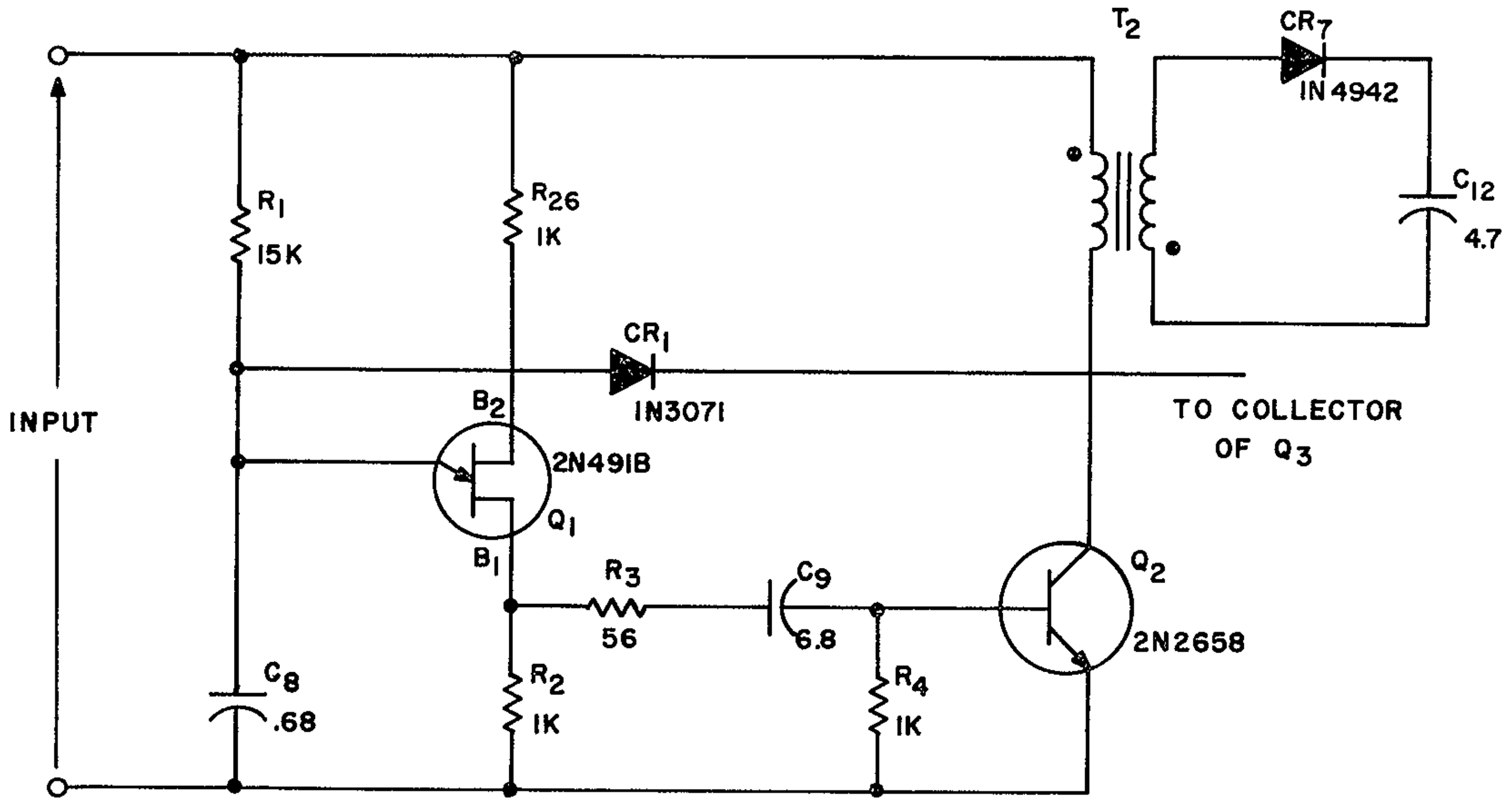

NOTE: ALL VALUES ARE IN OHMS, MICROFARADS, OR MICROHENRIES.

Fig. 13--Complete Starting Circuit.

for the differential input of the μA709. The bias is obtained by using a temperature compensated, 9-volt reference diode. The diode also provides a reference voltage for the feedback circuit. The modified basic diagram is shown in Figure 14.

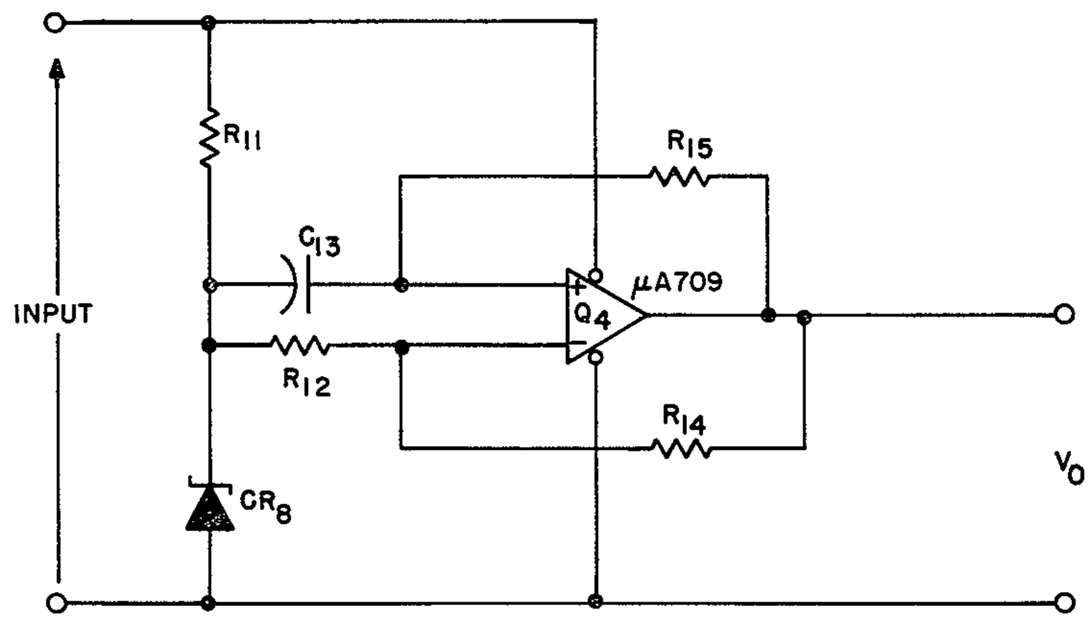

Fig. 14--Modified Basic Diagram of the Astable Multivibrator.

Resistors R_{12}, R_{14}, and R_{15} and capacitor C_{13} are used to establish the pulse width and repitition rate of the multivibrator. C_{13} is used to control the on time of the switching power transistor Q_3. Because of changing characteristics from component to component, the value of C_{13} is selected for each converter.

For the μA709 integrated circuit, the minus sign indicates the inverting input while the plus sign indicates the non-inverting input. The voltage transfer characteristic[6] is shown in Figure 15.

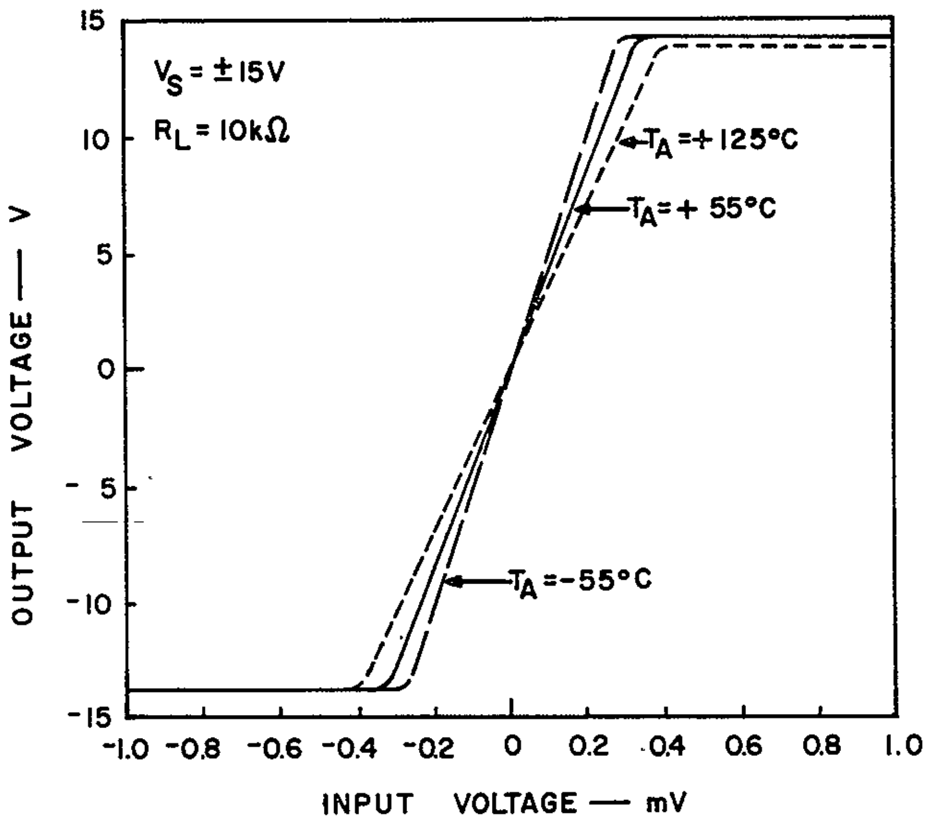

Fig. 15--Voltage Transfer Characteristic for the μA709.

This curve indicates that approximately ± 0.4 millivolt is required to switch the μA709 from the non-conducting state to the conducting state. The 0.4 millivolt is referenced to the non-inverting input;

i.e., if the inverting input rises 0.4 millivolt above the non-inverting input, the µA709 will switch to the conducting state.

For the integrated circuit to properly control the output voltage, a feedback path from the output voltage to the inverting input is needed. The feedback required is a continuous action degenerative feedback. The feedback path is shown in Figure 16 and consists of R_9, R_{10}, and an inhibit diode CR_6. CR_6 is included in the feedback path to inhibit the free running action of the integrated circuit Q_4. During the time Q_4 is in the conducting state, C_{13} is discharged through R_{16} and CR_9 in parallel with R_{15}. When the inverting input reduces to 9 volts less the diode drop, CR_6 becomes forward biased. The inverting input voltage then decreases at a rate equal to the RC time constant of the storage capacitor C_7 and the load resistance. This action causes the frequency to be modulated as a function of the load.

The maximum output power obtainable may be limited unless the discharge time of C_{13} is slightly less than the charge time. If the initial discharge time of C_{13} is the same as the charge time, the maximum frequency of operation is reduced slightly, and the maximum output power obtainable is decreased. A resistor diode network consisting of R_{16} and CR_9 is paralleled with the feedback resistor R_{15}. This will provide an initial discharge time slightly less than the charge time. The operating frequency will increase, and the required output power is now obtainable.

Figure 16 is a complete schematic diagram of the integrated control oscillator including the feedback circuit, the secondary portion of

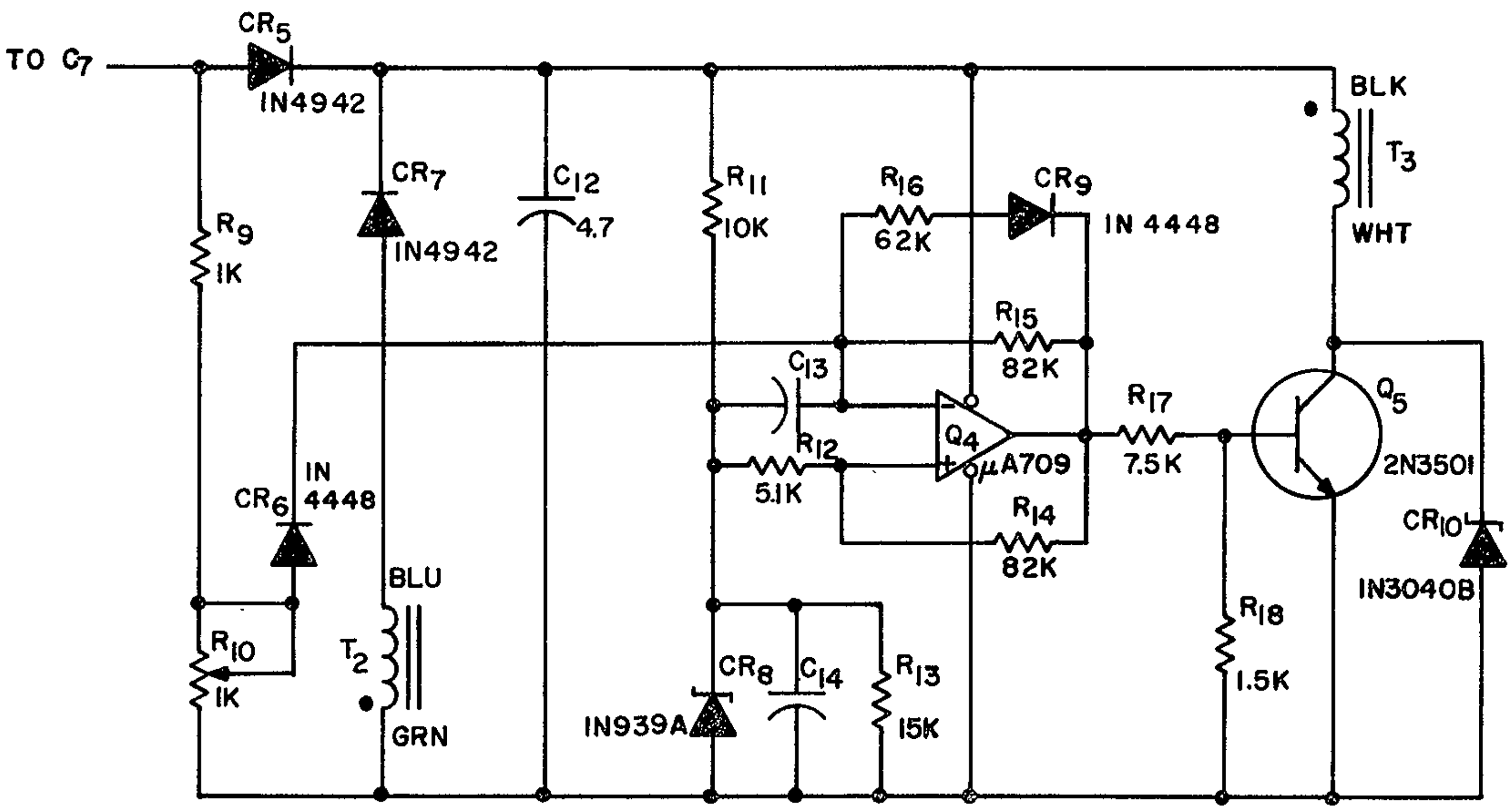

NOTE: ALL VALUES ARE IN OHMS, MICROFARADS, OR MICROHENRIES.

Fig. 16--Complete schematic Diagram of the Integrated Control Oscillator.

the starting circuit, and the output stage. The output stage consists of R_{17}, R_{18}, Q_5, CR_{10} and the pulse transformer T_3. R_{17} and R_{18} are bias resistors, and CR_{10} is a 68-volt zener diode included to protect Q_5 from voltage transients caused by the leakage inductance of T_3. The pulse transformer is used to provide the base signal to the switching power transistor Q_3. The transformer maintains the required output isolation.

D. Series Regulator

The complete series regulator is shown in Figure 17. The sampling circuit consists of the resistors R_{23}, R_{24}, and R_{25}. The differential amplifier, Q_9, acts as the comparator and error amplifier, while the reference diode CR_{11} provides the reference voltage. A low-voltage bias supply is provided by winding N_3 of transformer T_1, diode CR_3, and capacitor C_{10}. The series element is transistor Q_8 in conjunction with transistor Q_7 which form a Darlington pair. Transistor Q_6 provides current to the Darlington pair and to the comparator side of the differential amplifier.

To increase the stability of the regulator, capacitor C_{15} is used to provide a high-frequency cutoff and decrease the output impedance at high frequencies. Choke L_4 and capacitor C_{16} are added to provide a pi-filter output for the regulator.

The series regulator provides the desired regulation. This results in a slight decrease in efficiency and must be considered in estimating the overall efficiency of the converter.

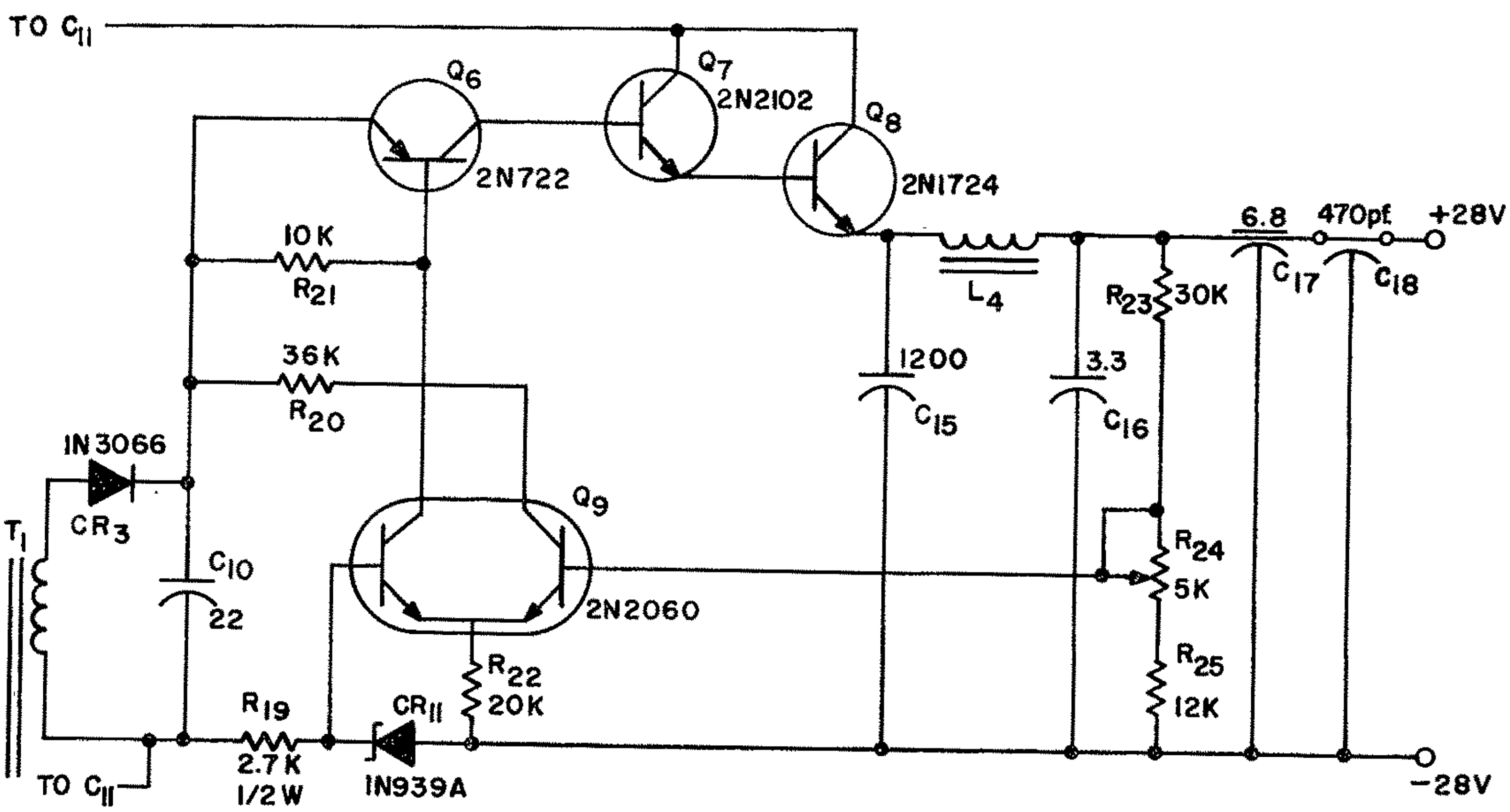

NOTE: ALL VALUES ARE IN OHMS, MICROFARADS, OR MICROHENRIES.

Fig. 17--Complete Series Regulator.

E. Radio-Frequency Interference Considerations

For the single-ended switching dc to dc converter to qualify for space applications, it must undergo electromagnetic compatibility tests. These tests indicate the ability of all individual vehicle electronic subsystems to operate simultaneously without performance degradation in accordance with the tests[7] listed below.

1. System electromagnetic compatibility tests.
2. Subsystem interference tests
3. Subsystem susceptibility tests.

The ability of electronic equipment to pass such tests is largely dependent upon the electronic packaging of the equipment. Since the converter is only a prototype and not in a final package form, the only tests performed are the "conducted interference tests" of (2) and (3) above. The tests performed are listed below.

1. Power line broad-band conducted interference.
2. Power line narrow-band conducted interference.
3. Audio susceptibility.

Broad-band interference[7] is defined as an interference signal with a bandwidth much greater than the bandwidth of the measurement equipment in use. Narrow-band interference[7] is ideally a single frequency, is sharply tunable, and has a spectrum that occupies a small part of the bandwidth of the measurement equipment. Susceptibility[7] is defined as that characteristic which causes equipment to malfunction or produce an undesirable response when subject to undesired electromagnetic voltages and fields. In the audio susceptibility test, a 3-volt rms sine wave with a frequency ranging from 50 Hz to 15,000 Hz is impressed upon the input of the test specimen. The output is monitored with an oscilloscope.

The input and output filters were incorporated in the final design specifically to enhance the electromagnetic compatibility of the converter. The input filter consists of the chokes L_1 and L_2 and the capacitors C_1, C_2, C_3, C_4, and C_5. The 470-picofarad capacitors, C_1 and C_2, serve as input voltage terminals and aid in shorting some of the higher radio-frequency signals to ground. The output filter is connected to the output of the series regulator and consists of choke L_4 and capacitors C_{15}, C_{16}, C_{17}, and C_{18}. The 470-picofarad capacitor, C_{18} is also used as an output voltage terminal. The values of capacitance and inductance used in the filters were determined experimentally.

A complete schematic diagram of the single-ended switching dc to dc converter is shown in Figure 18. A parts list for the converter is given in Appendix B.

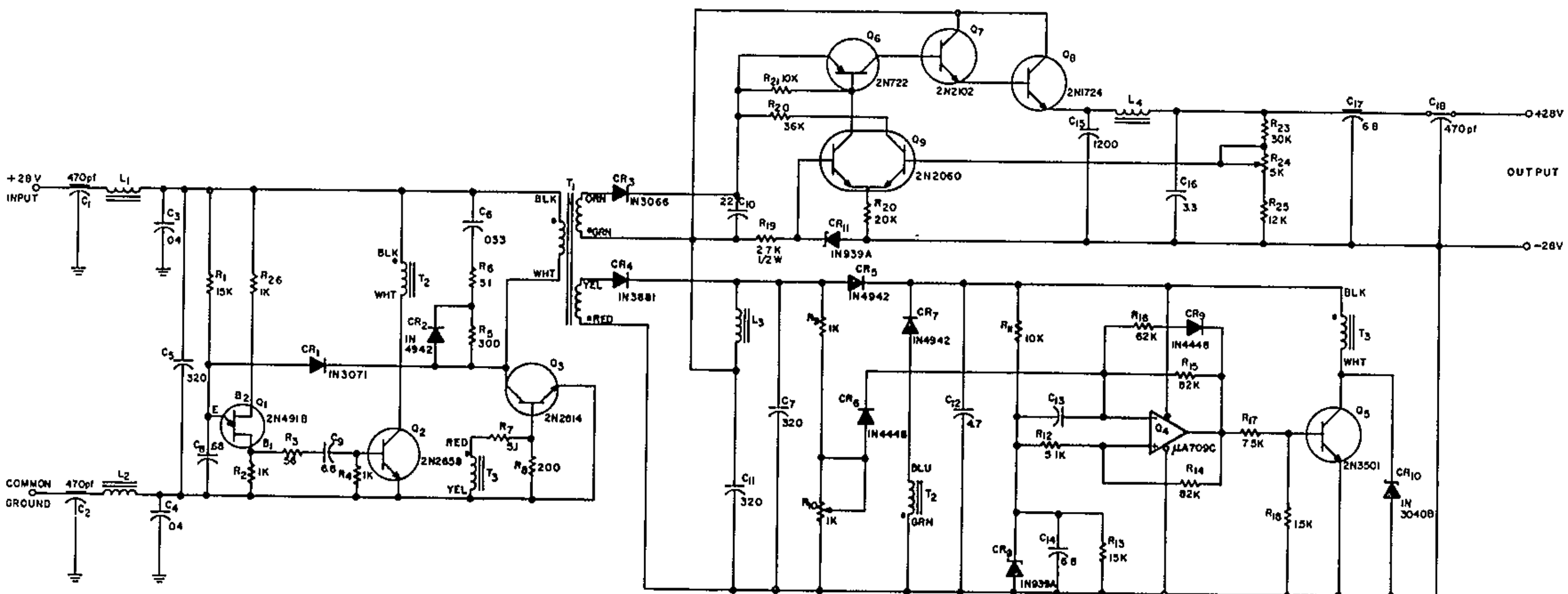

NOTE ALL VALUES ARE IN OHMS OR MICROFARADS UNLESS OTHERWISE INDICATED
C_{13} = 4300pf TEST SELECT

FIG. 18 -- COMPLETE CIRCUIT DIAGRAM OF THE SOLID-STATE SINGLE-ENDED SWITCHING DC TO DC CONVERTER

IV. CONVERTER PREFORMANCE

The converter was designed and a prototype constructed according to the specifications and conditions given. Several tests were conducted to insure that all of the design specifications were met.

Data for the input and output parameters were recorded at -21 degrees C, +23 degrees C, and +85 degrees C. The data are presented in Tables 1, 2, and 3. Ample time was allowed for the temperature to equalize before each reading was recorded.

The starting ability of the converter was checked over a temperature range of -25 degrees C to +85 degrees C. The converter started each time power was applied.

The output voltage change as a function of load current is shown in Figure 19. The curves are plotted for a nominal input voltage of 28 volts and consider the entire temperature range. The results for input voltages of 24 and 32 volts are very similar.

The d-c regulation may be found by using the equation[8]

$$\text{\% d-c regulation} = \frac{V_{NL} - V_{FL}}{V_{FL}} \times 100\% \qquad (40)$$

where V_{NL} is the no-load voltage and V_{FL} is the full-load voltage. The total d-c regulation considering temperature change, input voltage change, and load change is found to be 0.649 per cent or approximately $\pm$ 0.325 per cent. This is well within the design specification of $\pm$ 0.4 per cent.

TABLE I

INPUT AND OUTPUT PARAMETERS MEASURED AT -21 DEGREES C

Input Voltage (volts)	Input Current (amps)	Output Voltage (volts)	Output Current (amps)	Output Ripple (mv-pp)	Output Spikes (mv-pp)
	2.0	27.970	1.4	6.0	23.0
24.0	1.45	27.985	1.0	6.0	22.0
	—	28.034	0.0	1.0	18.0
	1.7	27.974	1.4	6.0	20.0
28.0	1.21	27.987	1.0	7.0	21.0
	—	28.034	0.0	2.0	19.0
	1.5	27.975	1.4	9.0	22.0
32.0	1.1	27.990	1.0	9.0	22.0
	—	28.035	0.0	2.0	20.0

TABLE 2

INPUT AND OUTPUT PARAMETERS MEASURED AT +23 DEGREES C

Input Voltage (volts)	Input Current (amps)	Output Voltage (volts)	Output Current (amps)	Output Ripple (mv-pp)	Output Spikes (mv-pp)
	2.0	27.927	1.4	5.0	12.0
24.0	1.41	27.938	1.0	5.0	12.0
	0.1	27.991	0.0	1.0	12.0
	1.7	27.928	1.4	5.0	20.0
28.0	1.21	27.939	1.0	5.0	20.0
	0.1	27.992	0.0	2.0	20.0
	1.5	27.929	1.4	9.0	15.0
32.0	1.05	27.943	1.0	10.0	15.0
	0.1	27.993	0.0	2.0	14.0

TABLE 3

INPUT AND OUTPUT PARAMETERS MEASURED AT +85 DEGREES C

Input Voltage (volts)	Input Current (amps)	Output Voltage (volts)	Output Current (amps)	Output Ripple (mv-pp)	Output Spikes (mv-pp)
	2.0	27.853	1.4	2.0	9.0
24.0	1.4	27.918	1.0	2.0	9.0
	—	27.996	0.0	2.0	10.0
	1.62	27.884	1.4	2.0	15.0
28.0	1.2	27.922	1.0	5.0	15.0
	—	27.997	0.0	1.0	9.0
	1.45	27.903	1.4	2.0	10.0
32.0	1.1	27.925	1.0	16.0	10.0
	—	27.998	0.0	2.0	10.0

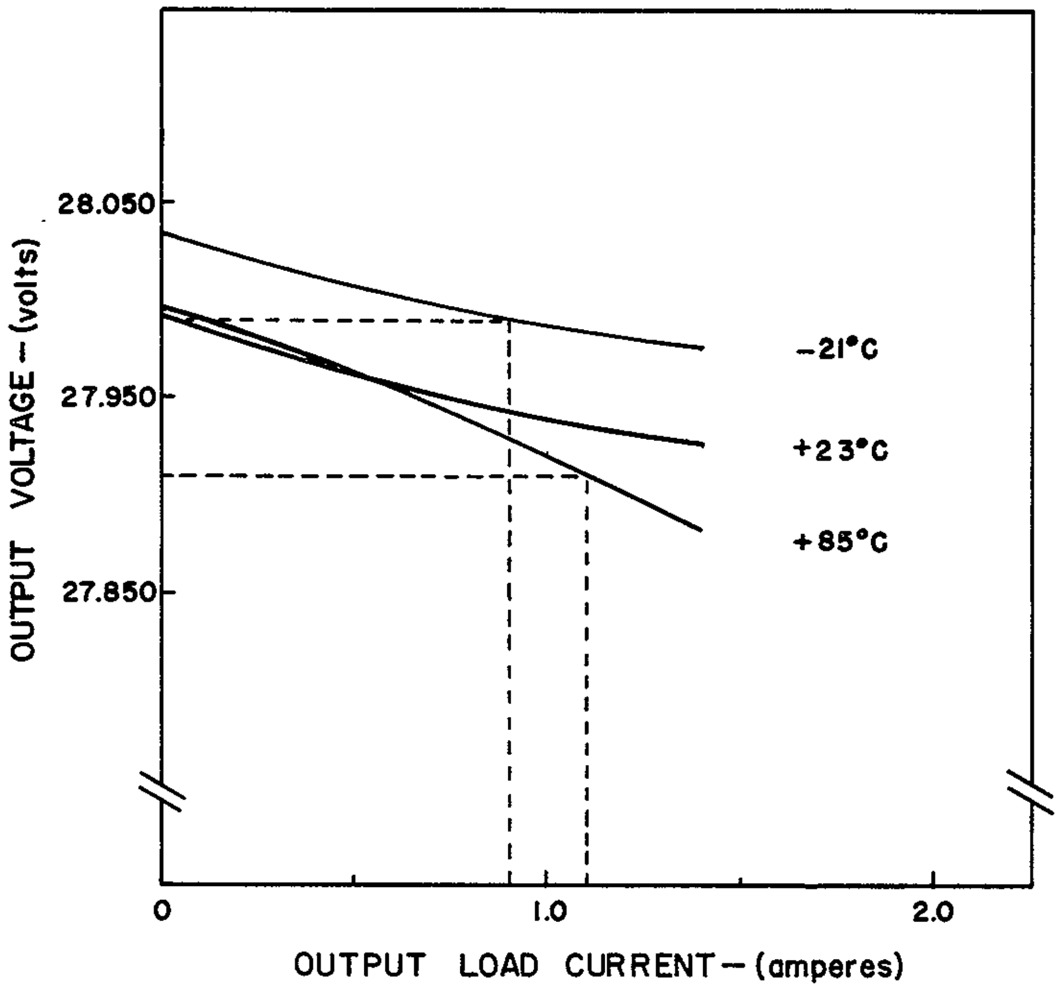

Fig. 19--Output Voltage Change as a Function of Load Change for an Input Voltage of 28 Volts.

For applications where a constant load is applied to the converter, the regulation is improved. The regulation for a $\pm$ 100-milliampere load change may be approximated from Figure 19 to be 0.27 per cent or approximately $\pm$ 0.14 per cent.

The converter efficiency for various input voltages as a function of temperature is given in Figure 20. An efficiency of approximately 80 per cent is maintained under all conditions of operation. This is much better than equivalent power conversion systems, which normally range from 65 to 70 per cent efficient.

The d-c output impedance of a power source is a measure of its ability to deliver power. The d-c output impedance may be calculated from the equation[8]

$$\text{d-c output impedance} = \frac{V_{NL} - V_{FL}}{I_{FL}}, \tag{41}$$

where I_{FL} is the full-load current. Figure 21 shows this output impedance for various input voltages as a function of temperature. The maximum output impedance calculated was 0.1021 ohms. Under normal operating conditions the output impedance is 0.0457 ohms.

The data recorded for the power line conducted interference tests are presented in Table 4. Figure 22 presents the broad-band conducted interference level for the positive and negative input lines. Figures 23 and 24 present the narrow-band conducted interference level for the positive and negative input lines, respectively. The MIL-I-6181D

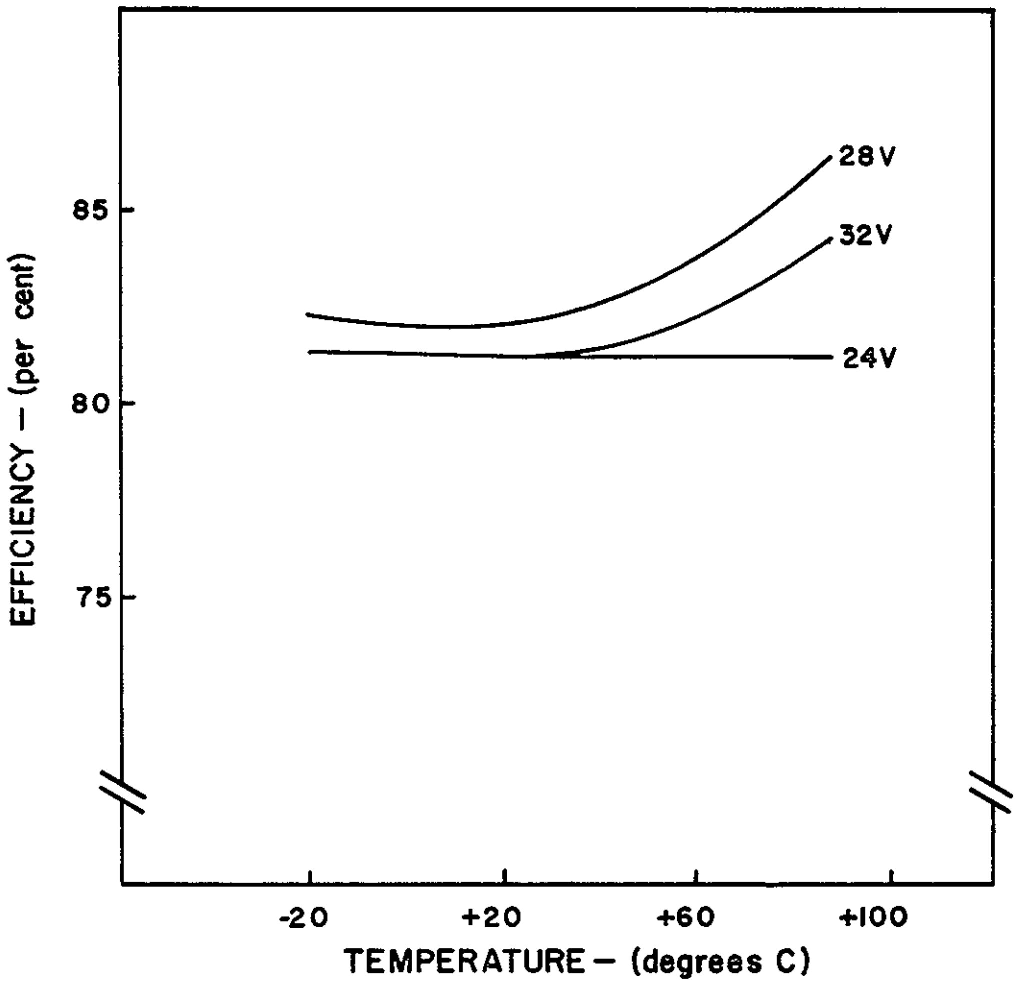

Fig. 20--Efficiency as a Function of Temperature for a Varying Input and Maximum Load Current.

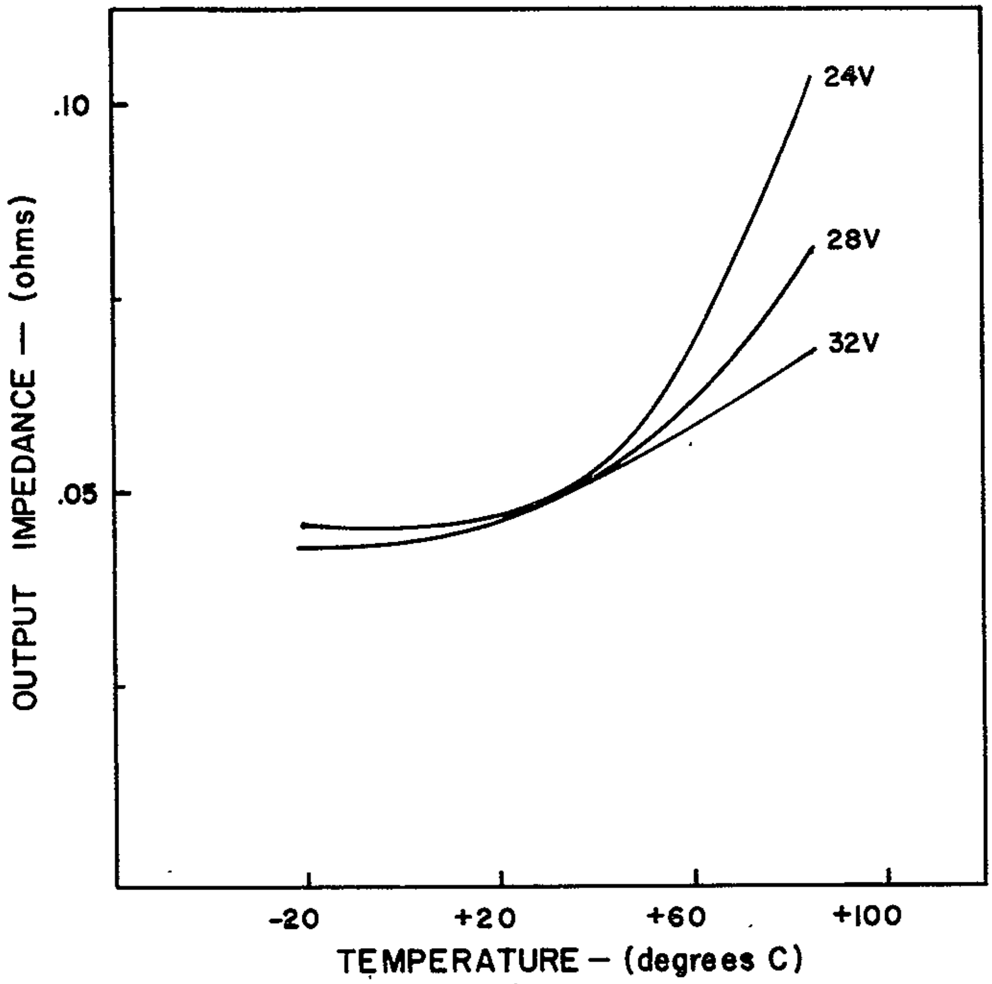

Fig. 21--Output Impedance as a Function of Temperature for a Varying Input Voltage and Maximum Load Current.

TABLE 4

DATA RECORDED FOR POWER LINE CONDUCTED INTERFERENCE TEST

POSITIVE 28 VOLT INPUT LINE			NEGATIVE 28 VOLT INPUT LINE		
FREQUENCY (megahertz)	BROADBAND (db above one microvolt/MHz)	NARROWBAND (db above one microvolt)	FREQUENCY (megahertz)	BROADBAND (db above one microvolt/MHz)	NARROWBAND (db above one microvolt)
0.150	89	41	0.150	98	51
0.152	95	49	0.212	95	50
0.215	93	47	0.350	92	44
0.350	88	41	0.500	89	
0.454	83	40	0.700	86	
0.580	82		1.000	82	
0.800	79		1.520	76	
1.000	77		2.000	73	
1.510	71		3.000	58	
2.000	69		4.500	71	
3.300	66		5.200	77	
5.000	75		6.000	60	
5.200	80		6.500	64	
4.500	73		8.800	66	
6.000	65		9.200	57	
6.900	61		10.000	68	
9.800	58		11.300	72	
11.000	62		15.000	57	
15.500	55		15.500	61	
25.000	45		17.000	63	
			24.000	58	

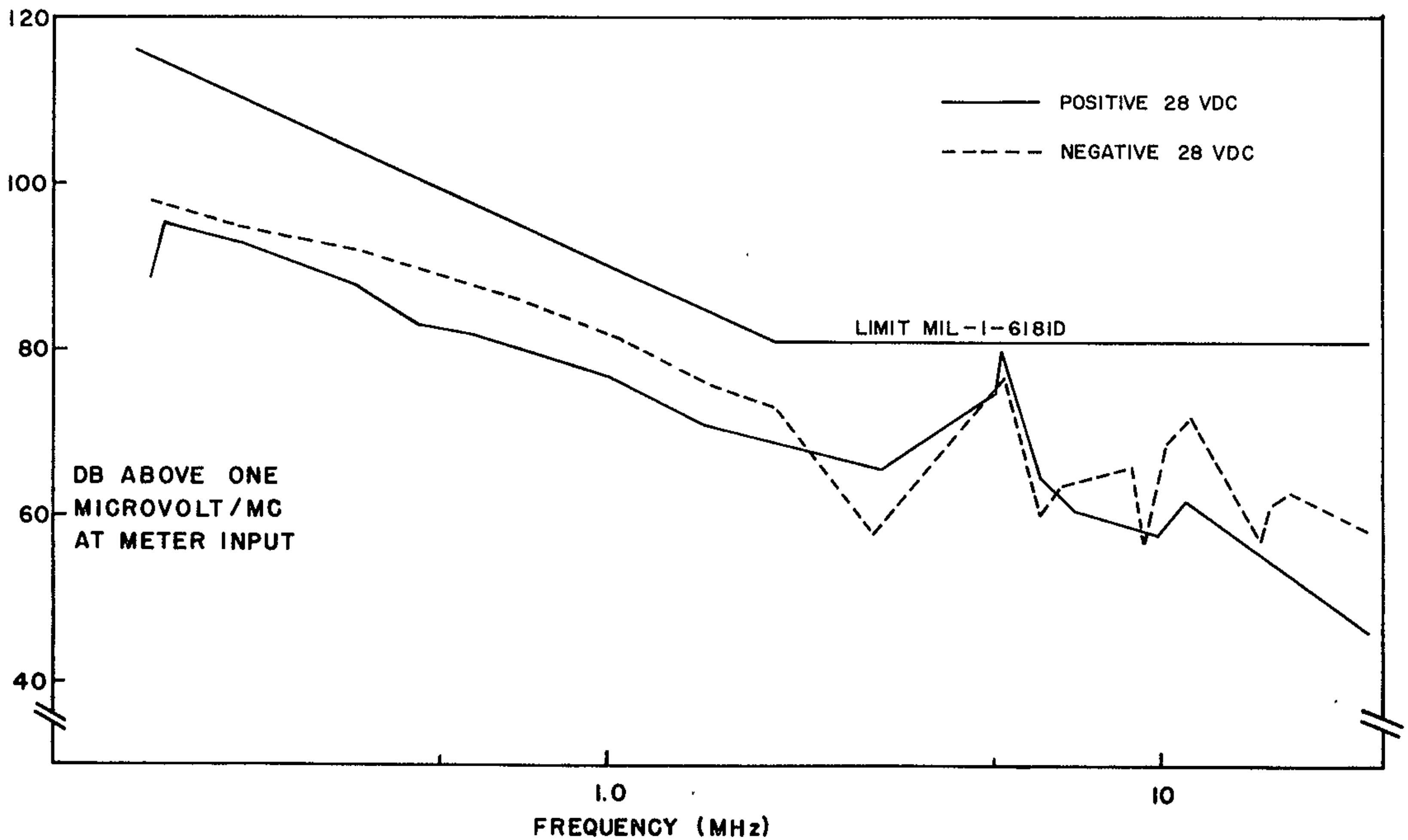

Fig. 22--Broad-band Conducted Interference Levels for Positive and Negative Input Lines.

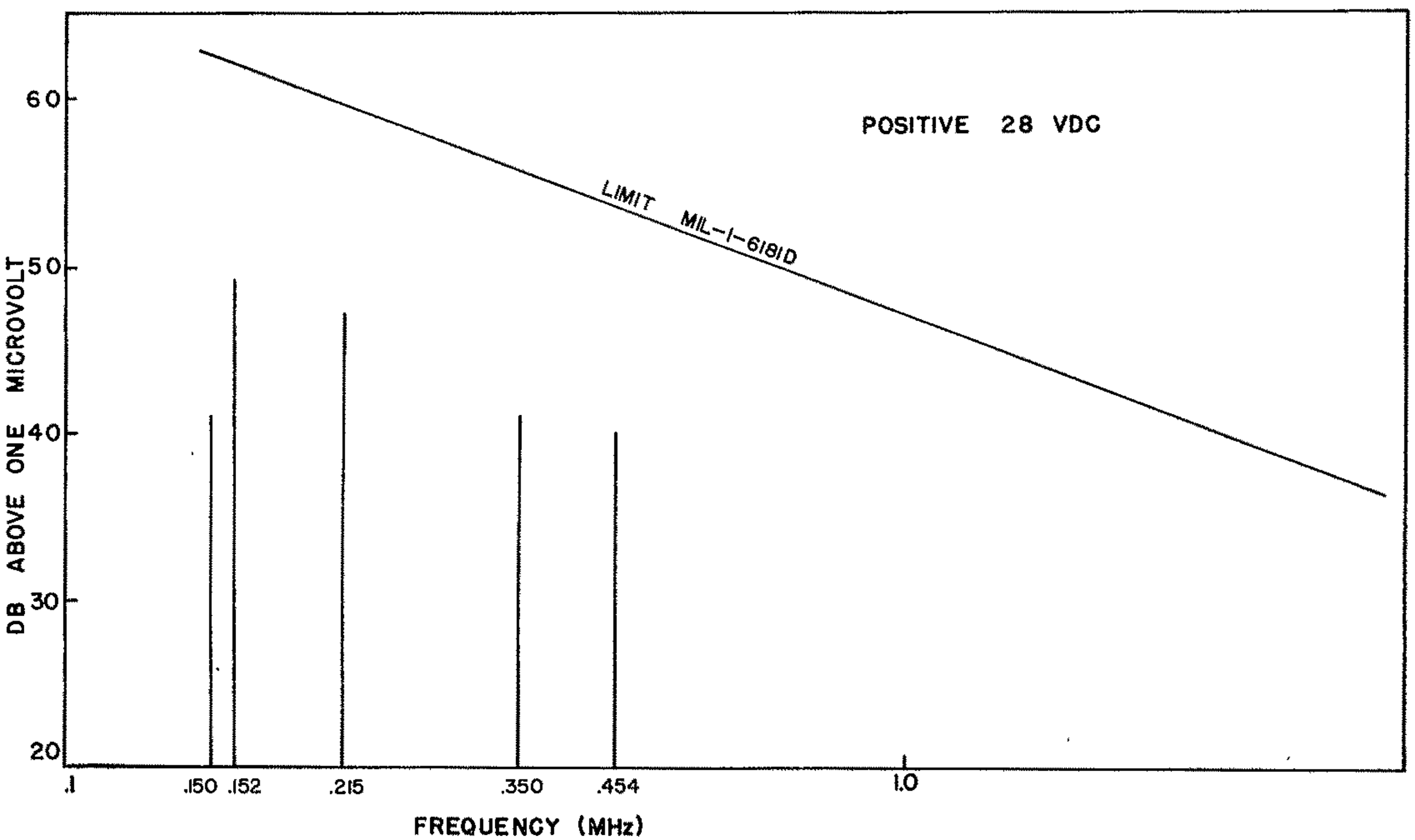

Fig. 23--Narrow-band Conducted Interference Level for Positive Input Line.

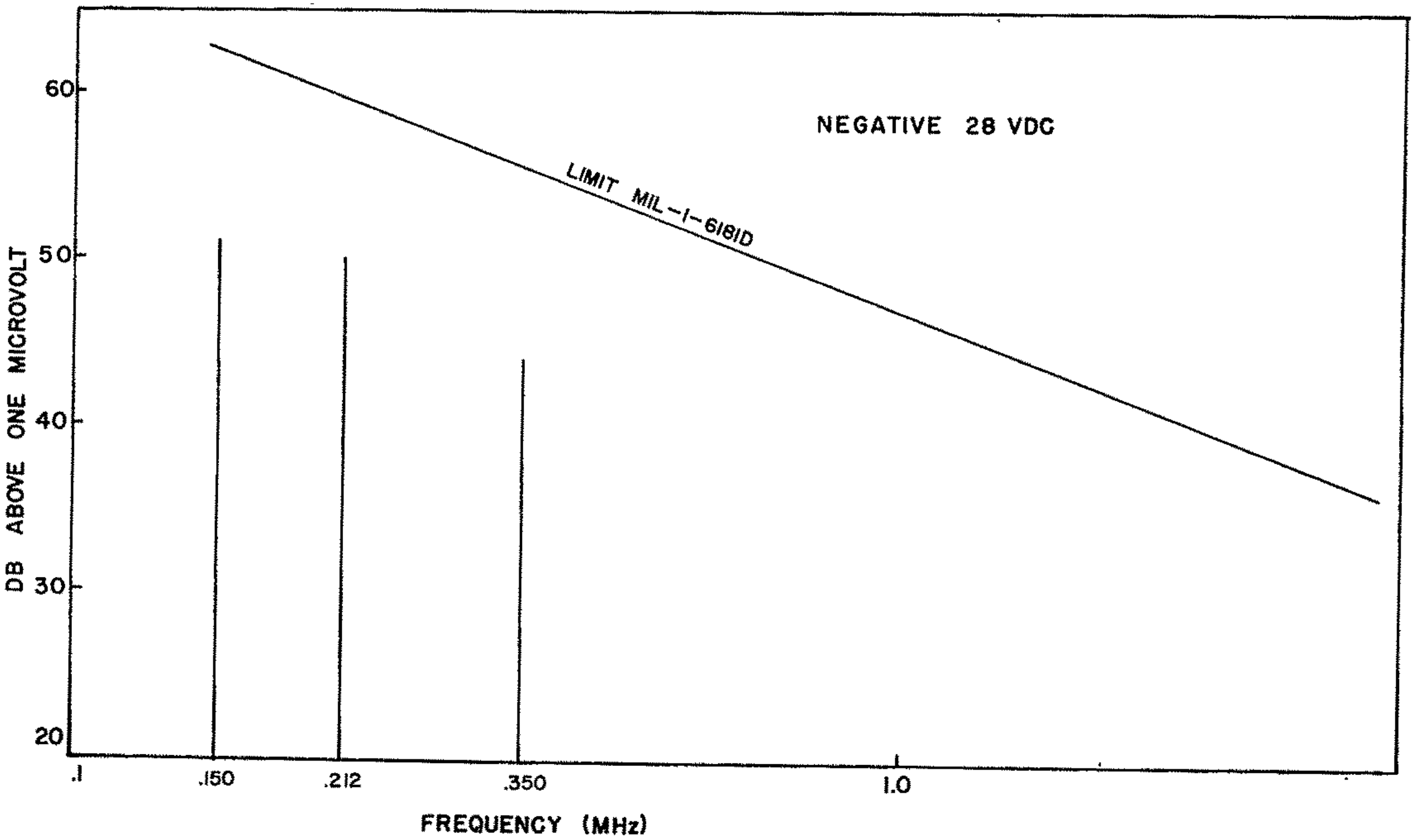

Fig. 24--Narrow-band Conducted Interference Level for Negative Input Line.

interference level is shown in Figures 22, 23, and 24. The interference level of the converter was well below the limit specified by MIL-I-6181D, except at a frequency of 5.2 megacycles. The interference level may be reduced further by the final design of the electronic package.

In the audio susceptibility test, a 3-volt rms sine wave with a frequency ranging from 50 Hz to 15,000 Hz was impressed upon the input terminals of the converter. There was no degradation of the output voltage throughout the above range.

V. CONCLUSIONS

The results of the tests performed on the converter indicate that it met all of the design specifications. The output voltage remained well within the regulation range of $\pm$ 0.4 per cent. The regulation was greatly improved for constant load applications. The ability of the converter to deliver power is shown by the low d-c output impedance.

The single-ended switching dc to dc converter displayed several distinct advantages over equivalent d-c power sources. For example, the converter provides a high operating efficiency with a reduction in size and weight. The reduction in size and weight is realized because of the simplicity of the power conversion circuit. The single-ended configuration facilitated the complete elimination of current transients. The current and voltage peaks on the primary and secondary of the isolation transformer and on the power transistor, Q_3, may be precisely controlled. This feature allows circuit components to be operated at a controlled stress level, which results in a significant increase in reliability.

It is most important to note that the single-ended switching dc to dc converter can provide a highly regulated, electrically isolated d-c output voltage with only one power stage. Equivalent power sources normally require two, or more, stages with a significant increase in components.

REFERENCES

1. J. F. Howell, "Ringing Choke Simplifies DC to DC Conversion," Electronics, Vol. 39, pp. 90-92, April 18, 1966.

2. J. Millman and H. Taub, Pulse, Digital, and Switching Waveforms, McGraw-Hill Book Company, Inc., New York, N. Y., 1965, pp. 65, 457-460.

3. W. H. Hayt, Jr. and J. E. Kemmerly, Engineering Circuit Analysis, McGraw-Hill Book Company, Inc., New York, N. Y., 1962, p. 342.

4. Permalloy Powder Cores, Data Catalog PC-303R Magnetics Inc., Butler, Pennsylvania, pp. 4, 8, 56-57.

5. B. D. Jimerson, "Feedback Techniques for Transistor Voltage Regulation," Electro-Technology, Vol. 71, pp. 76-79, March, 1963.

6. μA709 High Performance Operational Amplifier, Data Sheet, SL-64/A, Fairchild Semiconductor Products, April, 1966, pp. 1-3.

7. Electromagnetic Compatibility, George C. Marshall Space Flight Center, NASA, Specification, MSFC-SPEC-270, June 1, 1964, pp. 1, 97, 99, 101.

8. R. W. Landee, D. C. Davis, and A. P. Albrecht, Electronic Designers Handbook, McGraw-Hill Book Company, Inc., New York, N. Y., 1957, Chapter 15, p. 46.

9. G. V. Mueller, Introduction to Electrical Engineering, McGraw-Hill Book Company, Inc., New York, N. Y., 1957, pp. 259, 280.

APPENDIX A

The magnetic material selected for use in the single-ended switching transformer is powdered permalloy with a permeability, μ, of 60. This material can be shown to exhibit a constant inductance with a varying magnetomotive force. Considering a complete cross-sectional area of a core, the flux, Φ, is given by

$$\Phi = BA, \tag{A-1}$$

where B is the flux density and A is the cross-sectional area. Equation (A-1) may be differentiated with respect to the current i to yield.

$$\frac{d\Phi}{di} = A\,\frac{dB}{di} \tag{A-2}$$

The instantaneous emf, e, induced in an inductor may be expressed in two forms:[9]

$$e = N\,\frac{d\Phi}{dt}\,, \tag{A-3}$$

and

$$e = L\,\frac{di}{dt} \tag{A-4}$$

If equations (A-3) and (A-4) are equated, the inductance L is

$$L = N \frac{d\phi}{dt} \tag{A-5}$$

If equations (A-2) and (A-5) are combined, L becomes

$$L = NA \frac{dB}{di} \tag{A-6}$$

The magnetization curves[4] for powdered permalloy are shown in Figure A-1. The 60 μ material exhibits linear characteristics when plotted as a function of flux sensity, B, and magnetizing force H. This indicates that dB/di may be considered a constant since H is directly proportional to the current. Therefore, the inductance may be considered a constant for a varying magnetomotive force.

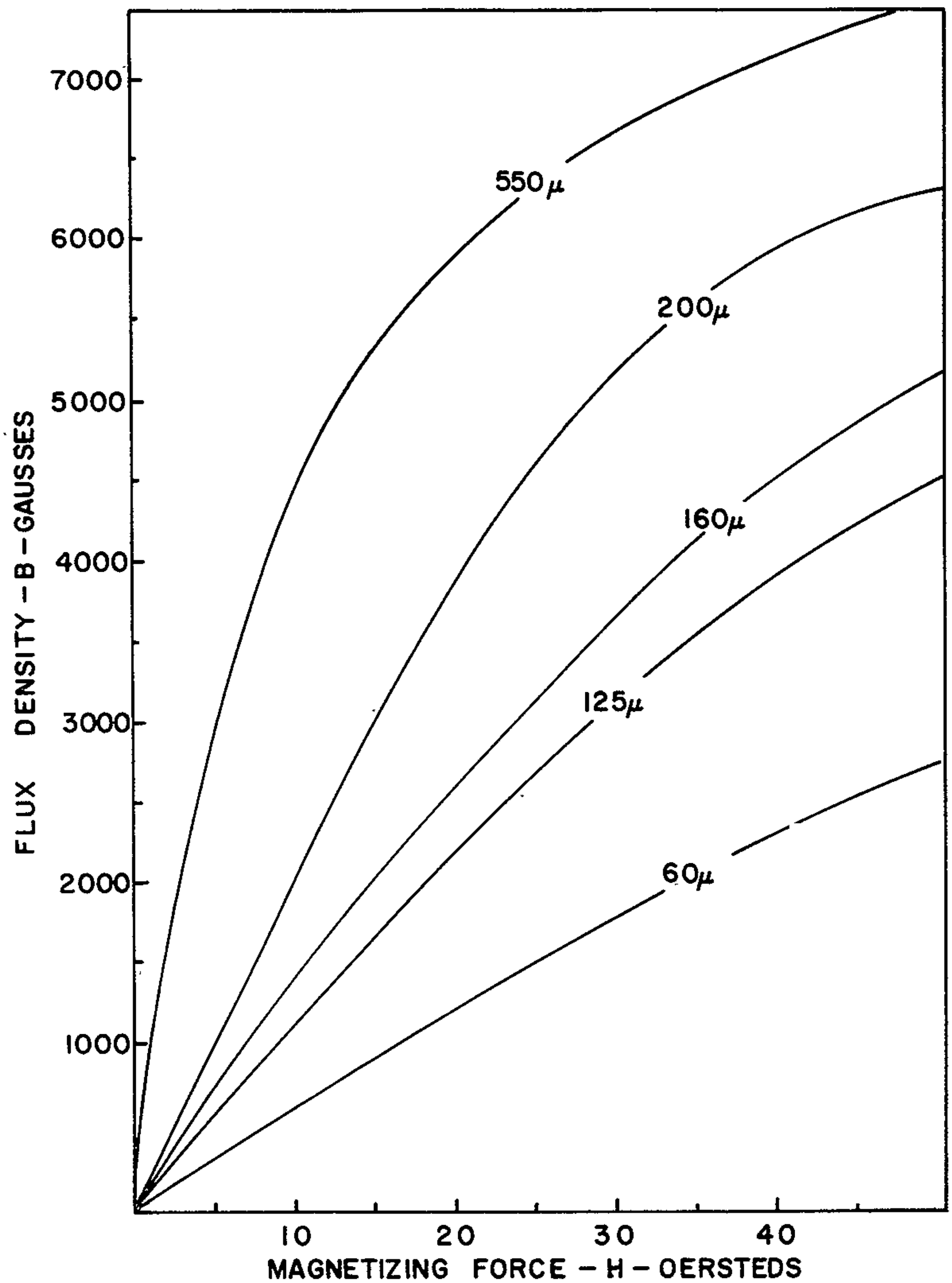

Fig. A-1--Magnetization Curves for Powdered Permalloy.

APPENDIX B

TABLE 5

SINGLE-ENDED SWITCHING DC TO DC CONVERTER PARTS LIST

Reference Symbol	Description
R_1	Fixed resistor, 15,000 ohms, 5%, 1/4 watt
R_2	Fixed resistor, 1,000 ohms, 5%, 1/4 watt
R_3	Fixed resistor, 56 ohms, 5%, 1/4 watt
R_4	Same as R_2
R_5	Fixed wirewound resistor, 300 ohms, 5%, 3 watt
R_6	Fixed wirewound resistor, 5.1 ohms, 5%, 3 watt
R_7	Same as R_6
R_8	Fixed resistor, 200 ohms, 5%, 1/4 watt
R_9	Same as R_2
R_{10}	Potentiometer, 1,000 ohms, 1 watt
R_{11}	Fixed resistor, 10,000 ohms, 5%, 1/4 watt
R_{12}	Fixed resistor, 5,100 ohms, 5%, 1/4 watt
R_{13}	Same as R_1
R_{14}	Fixed resistor, 82,000 ohms, 5%, 1/4 watt
R_{15}	Same as R_{14}
R_{16}	Fixed resistor, 62,000 ohms, 5%, 1/4 watt

TABLE 5--Continued

Reference Symbol	Description
R_{17}	Fixed resistor, 7,500 ohms, 5%, 1/4 watt
R_{18}	Fixed resistor, 1,500 ohms, 5%, 1/4 watt
R_{19}	Fixed resistor, 2,700 ohms, 5%, 1/2 watt
R_{20}	Fixed resistor, 36,000 ohms, 5%, 1/4 watt
R_{21}	Same as R_{11}
R_{22}	Fixed resistor, 20,000 ohms, 5%, 1/4 watt
R_{23}	Fixed resistor, 30,000 ohms, 5%, 1/4 watt
R_{24}	Potentiometer, 5,000 ohms, 1 watt
R_{25}	Fixed resistor, 12,000 ohms, 5%, 1/4 watt
R_{26}	Same as R_2
C_1	Fixed ceramic feedthru capacitor, 470 pF., 500 Vdc.
C_2	Same as C_1
C_3	Fixed mica capacitor, 0.04 μF., 100 Vdc.
C_4	Same as C_3
C_5	Fixed tantalum capacitor, 320 μF., 100 Vdc.
C_6	Fixed mica capacitor, 0.033 μF., 100 Vdc.
C_7	Same as C_5
C_8	Fixed tantalum capacitor, 0.68 μF., 35 Vdc.
C_9	Fixed tantalum capacitor, 6.8 μF., 35 Vdc.
C_{10}	Fixed tantalum capacitor, 22 μF., 35 Vdc.
C_{11}	Same as C_5
C_{12}	Fixed tantalum capacitor, 4.7 μF., 50 Vdc.

TABLE 5--Continued

Reference Symbol	Description
C_{13}	Test select
C_{14}	Same as C_9
C_{15}	Fixed tantalum capacitor, 1,200 μF., 50 Vdc.
C_{16}	Fixed tantalum capacitor, 3.3 μF., 50 Vdc.
C_{17}	Fixed tantalum feedthru capacitor, 6.8 μF., 35 Vdc.
C_{18}	Same as C_1
L_1	Choke, core 55121-M4, 60 turns, AWG No. 20
L_2	Same as L_1
L_3	Choke, core 55120-M4, 50 turns, AWG No. 19
L_4	Choke, core 55050-M4, 23 turns, AWG No. 19
T_1	Transformer, core 55071-M4
	Primary, 38 turns, AWG No. 17
	Secondary, 38 turns, AWG No. 17
	Secondary, 7 turns, AWG No. 24
T_2	Transformer, Core 55120-M4
	Primary, 153 turns, AWG No. 28
	Secondary, 153 turns, AWG No. 28
T_3	Transformer, core 55206-M4
	Primary, 900 turns, AWG No. 33
	Secondary, 166 turns, AWG No. 26
CR_1	Diode, 1N3071
CR_2	Diode, 1N4942

TABLE 5--Continued

Reference Symbol	Description
CR_3	Diode, 1N3066
CR_4	Diode, 1N3881
CR_5	Same as CR_2
CR_6	Diode, 1N4448
CR_7	Same as CR_2
CR_8	Reference diode, 1N939A
CR_9	Same as CR_6
CR_{10}	Zener diode, 1N3040B
CR_{11}	Same as CR_8
Q_1	Unijunction transistor, 2N491B
Q_2	Transistor, 2N2658
Q_3	Transistor, 2N2814
Q_4	Fairchild linear integrated circuit, μA709
Q_5	Transistor, 2N3501
Q_6	Transistor, 2N722
Q_7	Transistor, 2N2102
Q_8	Transistor, 2N1724
Q_9	Transistor, 2N2060

Notes:

All cores are Magnetic Inc. powdered permalloy.